

1. Report No. CR 120783	2. Government Accession No.	3. Recipient's Catalog No.	
4. Title and Subtitle PROPOSED DESIGN AND EXPERIMENTAL PERFORMANCE OF SHORT TWO DIMENSIONAL CURVED WALL DIFFUSERS UTILIZING SUCTION SLOTS		5. Report Date 9/3/71	6. Performing Organization Code
		8. Performing Organization Report No.	
7. Author(s) Tah-teh Yang and William G. Hudson		10. Work Unit No.	
9. Performing Organization Name and Address Mechanical Engineering Department Clemson University Clemson, South Carolina		11. Contract or Grant No. NAS3-13486	
		13. Type of Report and Period Covered Contractor Report	
12. Sponsoring Agency Name and Address National Aeronautics and Space Administration Washington, D.C. 20546		14. Sponsoring Agency Code	
15. Supplementary Notes Project Manager, Albert J. Juhasz Air Breathing Engines Division, NASA Lewis Research Center Cleveland, Ohio			
16. Abstract <p>The feasibility of designing short two-dimensional diffusers utilizing suction through one or more slots in the diffuser walls was investigated. Two wall contour designs were examined in several diffusers with area ratios of 2, 2.5, 3, and 4. For the first design a wall surface velocity distribution with all of the deceleration occurring in a concentrated region was prescribed. Based on this distribution a wall contour was computed using an ideal flow computer program. A suction slot was added in the region of deceleration to prevent flow separation under real flow conditions. Uniform exit velocity distribution and a diffuser effectiveness of 98% were achieved although only at suction rates ranging from 12% to 45% of the inlet flow. The second design had contour walls of circular arc cross section. For this design the diffuser effectiveness for an area ratio of 2.5 increased continuously from 30% to 85% as the suction rate was increased from 0% to 10%. For an area ratio of 4, the highest effectiveness attained with the circular arc design was 72.5%.</p>			
17. Key Words (Suggested by Author(s)) Curved wall diffuser Suction slots Boundary layer control Diffuser design		18. Distribution Statement Unclassified- unlimited	
19. Security Classif. (of this report) Unclassified	20. Security Classif. (of this page) Unclassified	21. No. of Pages 74	22. Price* \$ 3.00

* For sale by the National Technical Information Service, Springfield, Virginia 22151

FOREWORD

The research described herein, which was conducted by the Mechanical Engineering Department of Clemson University, was performed under NASA Contract NAS3-13486. Project Managers were Dr. William H. Roudebush and Mr. Albert Juhasz of the Airbreathing Engines Division, NASA-Lewis Research Center.

TABLE OF CONTENTS

Section		Page
	FOREWORD	iii
	TABLE OF CONTENTS	iv
	ABSTRACT	vi
	SUMMARY	1
I	INTRODUCTION	2
	1.1 BACKGROUND	2
	1.2 OBJECTIVE	4
	1.3 SCOPE	4
II	SYMBOLS	5
III	ANALYSIS AND DESIGN	7
	3.1 CONCEPTUAL DESIGN	7
	3.2 GRIFFITH DIFFUSER	8
	3.3 COMPUTER DESIGN PROGRAM	10
	3.4 COMPUTER ANALYSIS PROGRAM	12
	3.5 CIRCULAR ARC DIFFUSER	14
IV	APPARATUS AND INSTRUMENTATION	16
	4.1 TEST FACILITY	16
	4.2 GRIFFITH DIFFUSER GEOMETRY	17
	4.3 CIRCULAR ARC DIFFUSER GEOMETRY	22
	4.4 INSTRUMENTATION AND MEASUREMENTS	25
V	TEST CONDITIONS AND PROCEDURES	28
	5.1 TEST CONDITIONS	28
	5.2 TEST PROCEDURE	30

Section		Page
VI	DISCUSSION OF RESULTS	33
	6.1 GRIFFITH DIFFUSER (FIRST DESIGN)	33
	6.2 GRIFFITH DIFFUSER (SECOND DESIGN)	33
	6.3 CIRCULAR ARC DIFFUSER	48
	6.3.1 SINGLE-SLOT DIFFUSER	48
	6.3.2 DOUBLE-SLOT DIFFUSER	56
	6.3.3 CIRCULAR ARC DIFFUSER SUMMARY	58
VII	CONCLUSIONS	62
	7.1 GRIFFITH DIFFUSER	62
	7.2 CIRCULAR ARC DIFFUSER	63
VIII	REFERENCES	65
	APPENDIX - PRELIMINARY PERFORMANCE TESTS ON CIRCULAR ARC DIFFUSERS	66
	DISTRIBUTION LIST	69

ABSTRACT

The feasibility of designing short two-dimensional diffusers utilizing suction through one or more slots in the diffuser walls was investigated. Two diffuser wall contour designs were examined in several diffusers with area ratios of 2, 2.5, 3 and 4. For the first design a diffuser wall surface velocity distribution with all of the required deceleration occurring in a concentrated region was prescribed. Based on this velocity distribution, a wall contour was computed using an ideal flow computer program. A suction slot was added in the region of deceleration to prevent flow separation under real flow conditions. The performance of several diffusers using this wall contour and having area ratios of 2, 3 and 4 was evaluated experimentally using air at near ambient pressure and temperature. Test results indicate that the inviscid flow theory used for the design method is justifiable if flow separation can be prevented by applying sufficient slot suction. High diffuser effectiveness and uniform exit velocity distribution were achieved although only at suction rates several times higher than the desired upper limit of 10 percent of inlet flow. Lowering the suction rate caused an abrupt decrease in effectiveness. The second design, also tested with and without slot suction, had contour walls of circular arc cross section. For this design the diffuser effectiveness for the optimum area ratio of 2.5 continuously increased from approximately 30 percent to 85 percent as the suction was increased from zero to the upper limit of 10 percent of diffuser inlet flow. For an area ratio of 4, the highest diffuser effectiveness attained with the circular arc design was 72.5 percent.

SUMMARY

This report presents results of an investigation concerning the design and testing of two-dimensional subsonic curved wall short diffusers. Two design concepts were studied. The first design was arrived at by prescribing the potential flow velocity along the diffuser wall to have a region of constant high velocity at the inlet, a region of constant low velocity at the exit, and a region of concentrated deceleration connecting the inlet and exit regions. Based on this velocity distribution the wall contour was computed using a potential flow computer program. A suction slot was added at the deceleration zone to prevent flow separation under real flow conditions. Sidewall suction was applied to maintain two-dimensional flow. A diffuser utilizing this concept was fabricated and tested using air at ambient conditions. Nearly uniform exit velocity distribution and 98% diffuser effectiveness were achieved. Good correlation was obtained between predicted and experimental values of wall pressure distribution and center-line air velocity distribution. However, suction rates up to four times that predicted and allowable in practical applications were required to achieve these results. Decreasing the suction rate below the required values caused an abrupt decrease in effectiveness. Experimental results to date indicate that the design of the suction slot is a critical parameter. Hence it may be possible to reduce the suction rate by improving the slot design.

The second diffuser investigated had walls of circular arc cross section because of its simplicity. It was found that when operating with exit area to inlet area ratio of 2.5 to 1, diffuser effectiveness was

improved from approximately 30% to 85% as the slot suction rate was increased from 0% to 10%. Although flow separation at some distance downstream of the suction slot occurred to some extent regardless of the suction rate applied, the exit plane velocity distribution would be acceptable in many applications. The use of one suction slot at 15° and a second at 50° from entrance was attempted for the case of exit area to inlet area ratio of 4 to 1. Poor performance resulted because of the inflexibility of slot locations and the lack of independent slot suction control.

SECTION I

INTRODUCTION

1.1 BACKGROUND

In an internal flow system, a diffuser is a transitional section which connects a flow passage having a smaller cross-sectional area to a flow passage of larger area. Two characteristics of a diffuser desired in most applications are that it:

- (1) provide a nearly uniform velocity distribution for the fluid entering the larger passage at the diffuser exit, and
- (2) transform most of the kinetic energy of the higher velocity upstream flow to potential energy in the form of a higher static pressure of the downstream flow. A uniform exit velocity distribution assures an effective transformation of the kinetic energy to static pressure. However, the converse is not always true.

A measure of the performance of a given diffuser is the ratio of the actual to the ideal increase in static pressure of the fluid passing through the diffuser. This ratio is referred to as the diffuser effectiveness, η .

Many of the diffusers now used have straight walls. Performance improvement devices such as vanes, airfoils, or vortex generators may be used. Curved wall diffusers are occasionally used to meet certain geometrical requirements such as accommodating necessary components of the flow system. On rare occasions the wall contour may be designed for aerodynamic reasons. An example is the diffuser used in the wind tunnel at Princeton University (Ref. 1) which utilizes trapped vortices with limited success.

Much of the research work on diffusers has been done on the straight-wall diffuser. The simple geometry makes possible a systematic parametric study. Often the results of this research are a set of performance maps (Ref. 2, 3) which serve as a guide for estimating the performance of a proposed diffuser and to anticipate the possibility of flow separation.

Unfortunately, diffuser performance decreases as the angle of divergence increases. If space limitations force a given diffuser design to fall in the separated flow region of the map, the consequences may be predicted but no solution is offered.

Considerable research has also been done with performance improving devices (Ref. 4, 5, 6) which may be used to recover a higher fraction of the kinetic energy and to reduce the region of flow separation.

If, however, one is faced with requirements which prohibit the use of such auxiliary devices, the use of diffuser wall suction has the potential for improving diffuser performance.

In 1952, L.R. Manoni (Ref. 7) made a detailed study of bell-channel diffusers employing slot suction for boundary layer control. He used an electrical analogy tank to determine the wall geometry and concluded that a high performance diffuser of area ratio 2 to 1 and 20° equivalent cone angle was feasible. (The equivalent cone angle is the included angle of a conical diffuser having the same ratios of exit area to inlet area and length to inlet diameter as the curved-wall diffuser.) However, a diffuser designed by this technique having area ratio of 4.25 to 1 and equivalent cone angle of 40° was susceptible to separation and stability problems unless operated with extremely high suction rates.

1.2 OBJECTIVE

The objective of the research effort described in this report was to attempt a new design approach leading to a short, two-dimensional diffuser having unseparated flow and uniform exit velocity distribution. This work should lay the foundation for the eventual design of axially symmetrical diffusers having the same desirable characteristics.

1.3 SCOPE

In order to achieve the objective, a research program was carried out to:

- (1) Use existing analyses and computer programs required in the design of flow channels with prescribed boundary conditions (inlet, exit, and wall velocity distributions).
- (2) Use existing analyses and computer programs for analyzing the channel flow field of a known geometry.

- (3) Utilize the analyses and programs of (1) and (2) to examine the following concepts:
- (a) a diffuser having the deceleration region along the wall concentrated in a narrow zone equipped with a suction slot in each wall.
 - (b) a diffuser having continuous deceleration along a circular arc wall, also provided with suction slots.
- (4) Fabricate and test diffusers having geometries resulting from the concepts stated in (3a) and (3b). Experimental tests included performance, velocity distributions, and pressure distributions to determine the validity of the configurations designed and the accuracy of the analyses.

SECTION II

SYMBOLS

A_{cs}	cross-sectional area
AR	area ratio, exit area to inlet area
C_p	pressure coefficient, $\frac{V_i^2 - V_z^2}{V_i^2}$
H_o	inlet height of diffuser
$H(z)$	local diffuser height
P	pressure
P_a	room atmospheric pressure
$P_{d,i}$	dynamic pressure at diffuser inlet

P_{loss}	pressure loss as a percentage of total inlet pressure
$P_{s,e}$	static pressure at diffuser exit
$P_{s,i}$	static pressure at diffuser inlet
$P_{t,i}$	total pressure at diffuser inlet
Q	fluid volume flow rate
Re No.	Reynolds number, $\left[\frac{(4 A_{cs} / \text{perimeter})(\text{velocity})}{\text{fluid kinematic viscosity}} \right]_{\text{diffuser inlet}}$
S	distance from diffuser inlet as measured along the curved wall
Slot suction	percentage of inlet flow removed through suction slots or suction holes
S.W. suction	sidewall suction as a percentage of inlet flow
Sp	spacing between bodies in a cascade
V	fluid velocity
V_i	velocity at diffuser inlet
V_e	velocity at diffuser exit
V_z	velocity at location z
V_∞	free stream fluid velocity
W	diffuser width
x	horizontal distance from diffuser sidewall in direction normal to sidewall
X	x/W
y	vertical distance above diffuser centerline
Y	$y/H(z)$
z	horizontal distance from diffuser inlet to a local X-Y plane
Z	z/H_o

η	diffuser effectiveness = $\frac{P_{s,e} - P_{s,i}}{P_{d,i} \left[1 - \left(\frac{1 - \% \text{ total suction}}{100} \right)^2 \right]}$
Φ	velocity potential
Ψ	stream function
θ	the angular direction of flow of velocity V

SECTION III

ANALYSIS AND DESIGN

3.1 CONCEPTUAL DESIGN

There are an infinite number of possible contours connecting a given flow passage to a larger one. Associated with each geometry, there is a pressure distribution along the wall which is theoretically predictable from potential flow theory assuming no separation and negligible boundary layer thickness.

There are two distinct possibilities with regard to the manner of handling the deceleration along the diffuser wall:

- (1) The deceleration may occur abruptly in a narrow region on the diffuser wall. This geometry is similar to that used on experimental high-lift laminar airfoils, originally suggested by A.A. Griffith as reported by Lachmann (Ref. 8) and is henceforth referred to as the Griffith diffuser.
- (2) Deceleration may occur continuously over the entire length of the diffuser wall.

The Griffith diffuser utilizes the first method and is discussed in paragraph 3.2. The circular arc diffuser was selected to represent the

second method because of its simple geometry and its short length. This case is discussed in paragraph 3.5.

3.2 GRIFFITH DIFFUSER

Consider dividing the walls of the diffuser into three regions as shown in Figure 1: a constant high velocity low static pressure upstream region, a constant low velocity high static pressure downstream region, and a rapidly decelerating region between.

By confining the troublesome adverse pressure gradient to a narrow zone, it may be possible to prevent separation by applying boundary layer control to this zone. One approach is placing a suction slot in this zone whereby flow separation due to the adverse pressure gradient may be avoided since the suction slot permits removal of the retarded fluid. This method of boundary layer control was first implemented in an experimental airfoil by M.B. Glauert (Ref. 9).

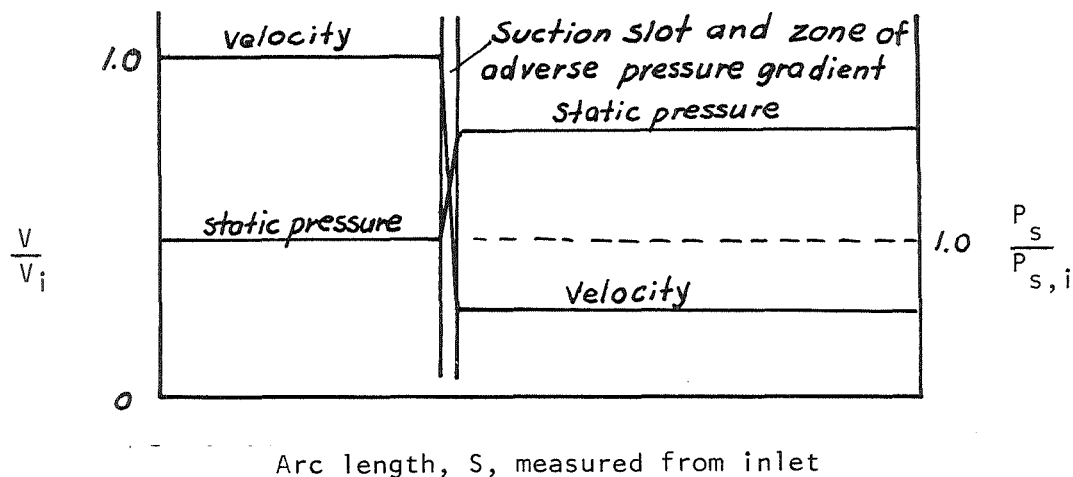


Figure 1. Velocity and pressure distributions along diffuser wall.

Sir Geoffrey Taylor's criterion for minimum suction requirement across a suction slot having a concentrated adverse pressure gradient is reported by Goldstein (Ref. 10). According to Taylor's criterion, the minimum amount of fluid within the boundary layer which must be removed is the quantity from the surface up to where

$$\frac{v_1}{V_1} = \sqrt{1.0 - \left(\frac{V_2}{V_1}\right)^2} \quad (1)$$

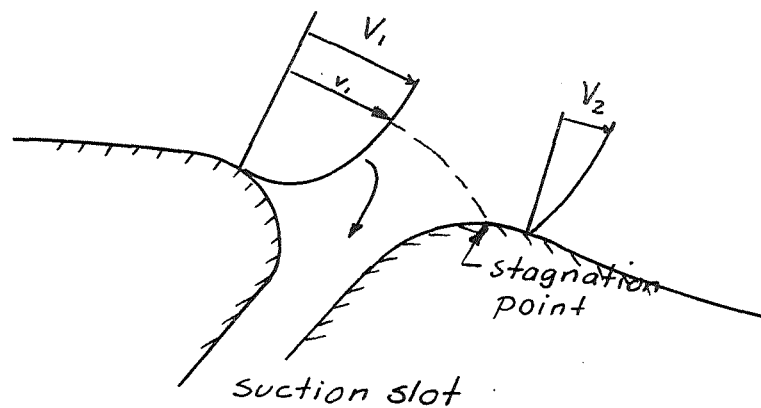


Figure 2. Flow in vicinity of slot.

V_1 and V_2 are the fluid velocities outside the boundary layers just upstream and downstream of the slot. v_1 is the fluid velocity within the boundary layer upstream of the slot as shown in Figure 2. Along streamlines near the contoured wall, deceleration is constrained to the region across the slot. For streamlines farther away from the contoured wall, the deceleration region becomes more spread out, and at the central core of the fluid, the deceleration extends over quite a large part of the diffuser length. Thus flow separation is prevented by using suction to overcome an

adverse pressure gradient along the solid walls of the diffuser. In estimating the required suction rate, the boundary layer velocity profile upstream of the slot is needed. Since the potential velocity upstream of the suction slot is prescribed to be nearly constant, the profile may be approximated as that existing on a flat plate. The geometry of the contoured wall can be obtained, assuming that the suction rate is sufficient to prevent flow separation, by solving the inverse problem, which is defined by prescribing the desired velocities at yet to be determined boundaries of the flow field.

3.3 COMPUTER DESIGN PROGRAM

This program deals with the problem of determining the channel geometry for prescribed inlet, exit, and wall velocity distributions using two-dimensional incompressible potential flow theory.

John D. Stanitz (Ref. 11) has shown that in a two-dimensional flow field, the magnitude of the flow velocity, V , and its direction, θ , can be expressed as functions of the stream function, Ψ , and the velocity potential, Φ . Letting the density of the fluid be 1.0, the equation of continuity for incompressible flow is

$$\frac{\partial \ln V}{\partial \Phi} + \frac{\partial \theta}{\partial \Psi} = 0 \quad (2)$$

and the equation of irrotational fluid motion is

$$\frac{\partial \ln V}{\partial \Psi} - \frac{\partial \theta}{\partial \Phi} = 0 \quad (3)$$

Combining equations (2) and (3) results in

$$\frac{\partial^2 \ln V}{\partial \Phi^2} + \frac{\partial^2 \ln V}{\partial \Psi^2} = 0 \quad (4)$$

Thus $\ln V$ satisfies the Laplace equation in the Φ - Ψ plane, and with a given set of boundary conditions, $\ln V$ may be found over the entire region.

The corresponding direction of flow, θ , may be found by integrating equation (3) as

$$\theta = \int_{\Psi} \frac{\partial \ln V}{\partial \Psi} d\theta \quad (5)$$

In designing the diffuser, one needs to know X and Y in terms of θ , V , and Φ or Ψ for the outermost streamlines in the physical plane. The relationships among X , Y , θ , V , Φ , and Ψ are:

$$X = \int_{\Psi} \frac{\cos \theta}{V} d\Phi, \quad \text{or} \quad X = -\int_{\Phi} \frac{\sin \theta}{V} d\Psi \quad (6)$$

$$Y = \int_{\Psi} \frac{\sin \theta}{V} d\Phi, \quad \text{or} \quad Y = \int_{\Phi} \frac{\cos \theta}{V} d\Psi \quad (7)$$

A digital computer program utilizing the Gauss-Siedel method with over-relaxation to speed convergence was utilized to solve equation (4). The program utilized numerical integration to solve for the coordinates of the various streamlines, including the outermost streamline which coincides with the channel wall geometry assuming the boundary layer thickness to be negligible.

3.4 COMPUTER ANALYSIS PROGRAM

This program considers the problem of determining the potential flow field about a given geometry. J.L. Hess and A.M.O. Smith (Ref. 12) of Douglas Aircraft Company developed the surface-source-distribution method for solving such a flow field. They have also developed a digital computer program which utilizes this technique to solve for the flow field about infinite two-dimensional cascades. By adding the stagnation streamlines, the flow channel of the two-dimensional diffuser may be analyzed as a cascade problem. See Figure 3.

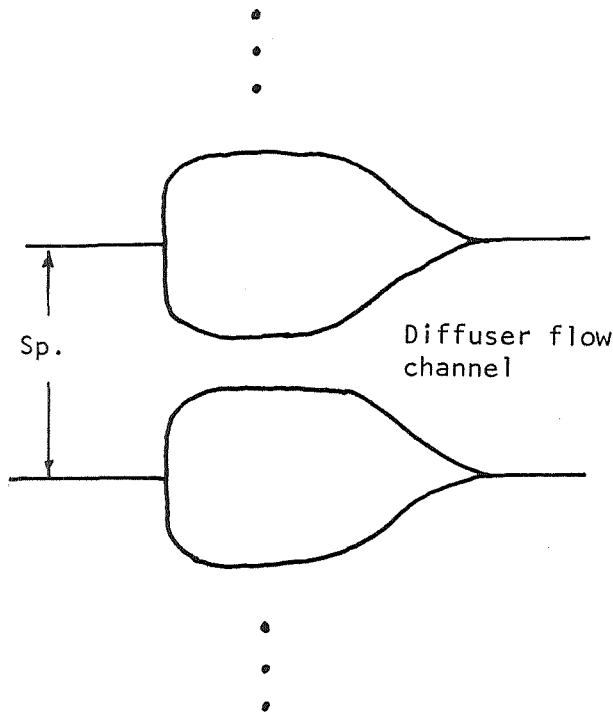


Figure 3. Body coordinates and body spacing define the diffuser flow channel.

After the geometry for a prescribed velocity distribution had been obtained by using the design program, the analysis program was used to

calculate the velocities along the surface of the resultant body. This procedure was followed to verify the diffuser contour design. Also the analysis program was used to yield the modified velocity distribution for various suction rates for both Griffith and circular arc diffusers. Suction flow was accounted for as follows. A non-uniform onset flow was input by specifying the normal and tangential velocities on all body elements. The tangential velocities were specified to be zero on all body elements. For elements with no suction, a zero normal velocity was specified. For elements with suction, a normal velocity was specified so as to yield the same total non-uniform onset flow as the 0° streamflow by applying the equation:

$$\begin{aligned} \text{Normal velocity for suction elements} \times \Sigma \text{ suction element lengths} \\ = \text{onset } 0^\circ \text{ streamflow velocity} \times \text{body spacing} \end{aligned}$$

or, since onset 0° velocity = 1.0,

$$\text{Normal velocity for suction elements} = \frac{\text{body spacing}}{\Sigma \text{ suction element lengths}}$$

A subroutine was added to the original computer program which combined 1%, 2%, ... , 10% of the computed non-uniform flow velocities with the computed 0° streamflow velocities to yield the resulting tangential velocities at each body element for suction rates from 1% to 10% in 1% intervals. X and Y components of off-body velocities were also obtained in this subroutine by combining the 0° streamflow off-body velocities with 1%, 2%, ... , 10% of the non-uniform off-body velocities.

3.5 CIRCULAR ARC DIFFUSER

Consider now the second method of dealing with the deceleration along the diffuser wall. A very simple geometry results if the diffuser walls consist of two circular arcs as shown in Figure 4. The wall velocity distribution from potential flow theory, with and without slot suction, is shown in Figure 5. Slot suction would shift the real flow separation point downstream.

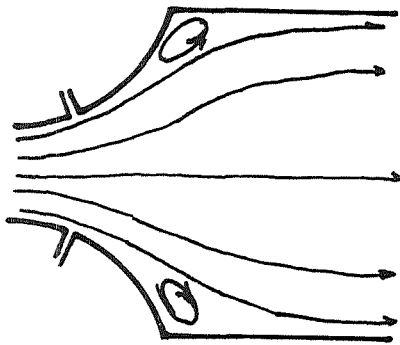


Figure 4. Circular arc diffuser with a single slot per wall.

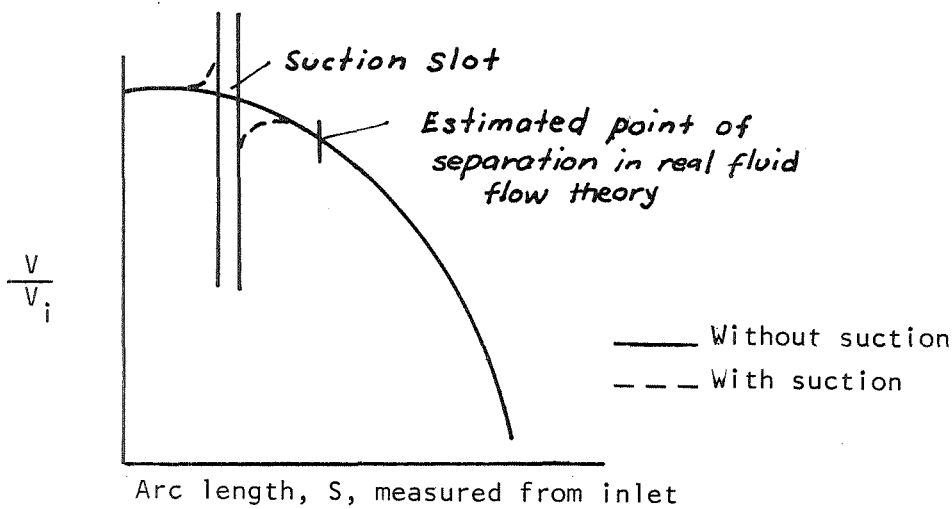


Figure 5. Wall velocity distribution (potential flow theory).

It may be possible to locate the slot so that a moderate rate of suction enables the flow to remain attached almost to the end of the circular arc. In this case a higher diffuser effectiveness should be expected.

For higher area ratios it is likely that more than one slot per diffuser wall will be required as shown in Figure 6. Figure 7 shows the resulting wall velocity distribution.

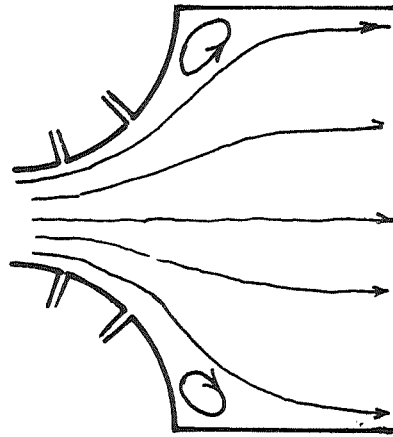


Figure 6. Circular arc diffuser (two slots per wall).

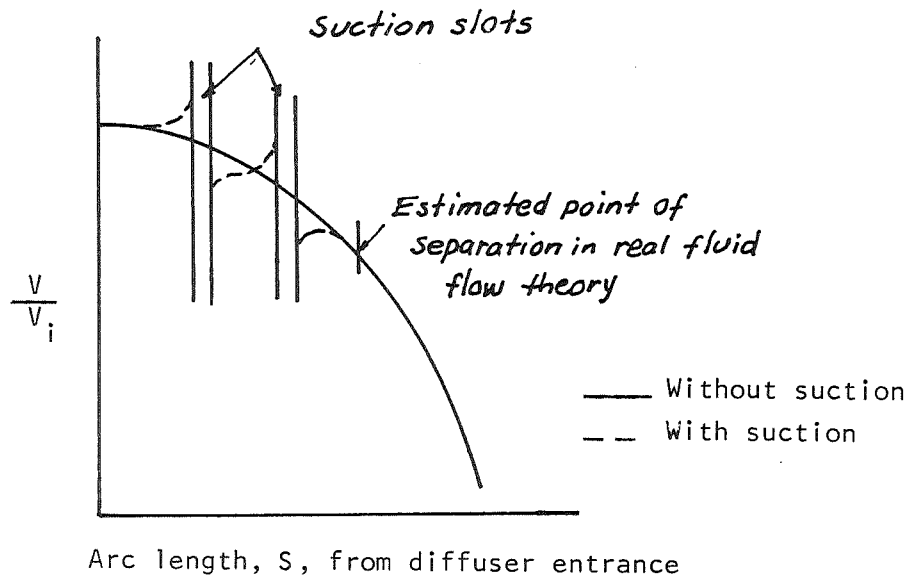


Figure 7. Wall velocity distribution (potential flow theory).

If slot suction is to be successful in preventing flow separation when used with a diffuser having continuous deceleration, the suction must exert an influence over an extended region both upstream and downstream of the slot. Also, an independent control of the suction rate through each slot would be required when the double-slot scheme is used for the case of high area ratio. This would tend to offset the advantage of geometrical simplicity.

SECTION IV

APPARATUS AND INSTRUMENTATION

4.1 TEST FACILITY

Two diffusers having wall profiles determined with the aid of the computer programs discussed in section III and five circular arc diffusers were fabricated and tested. These diffusers were fabricated from aluminum stock to tolerances within one-thousandth inch (.0025 cm). Diffuser sidewalls were fabricated from a sintered porous stainless steel sheet so that two-dimensional flow could be achieved by applying suction to each sidewall.

Tests were performed by attaching the test sections to a 24 inch (61 cm) circular plate located at the end of a 20 ft. (6.1 m) long duct delivering air from a 10,000 CFM ($4.720 \text{ m}^3/\text{sec}$) industrial fan. A shutter-type damper at the fan inlet was used to regulate the flow rate. Air delivery to the diffuser was made uniform and steady by flow-straightener tubes of 1 1/4 inch (3.18 cm) diameter, and four sets of fine screens of mesh sizes 20, 40, 50 and 100 per inch installed inside the duct. A positive displacement blower rated at 300 CFM ($0.142 \text{ m}^3/\text{sec}$) was used to

provide the sidewall and the slot suction required for the tests. Figure 8 shows the test arrangement pictorially and schematically.

4.2 GRIFFITH DIFFUSER GEOMETRY

The first of the two Griffith diffusers designed and fabricated failed to operate satisfactorily. Paragraph 6.1 discusses the probable reason for unsatisfactory performance. Figure 9 shows the coordinates and the profile resulting from the design program. As shown, a slot was cut normal to the surface in the zone of maximum deceleration. The surface velocity distribution which was prescribed to obtain the wall contour of Figure 9 is shown in Figure 10. Figure 11 shows the wall velocity distribution as predicted by the analysis program when suction at the rate of 10% of the inlet flow is applied to the zone of maximum deceleration.

The second Griffith diffuser is shown in Figure 12. A suction slot 0.05 inches (0.127 cm) wide was cut as indicated in the figure. By varying the spacing between the contoured walls, the diffuser could be operated at various area ratios. Figure 13 shows the wall velocity distribution which was prescribed to the design program to yield the second Griffith diffuser coordinates. A more rapid rate of deceleration was prescribed for the second diffuser as shown by comparing Figure 13 with Figure 10. This resulted in the cusp just downstream of the slot as observed in Figure 12.

Reference 12 shows that the spacing enters into the expression for the complex velocity on the surface in the form of a multiplication factor of the argument of a hyperbolic sine function. Thus a change of spacing results in changes of local surface velocities, but the profiles remain similar. Figure 14 shows the wall velocity distributions for area ratios of 2, 3, and 4 as predicted by the potential flow analysis program. The

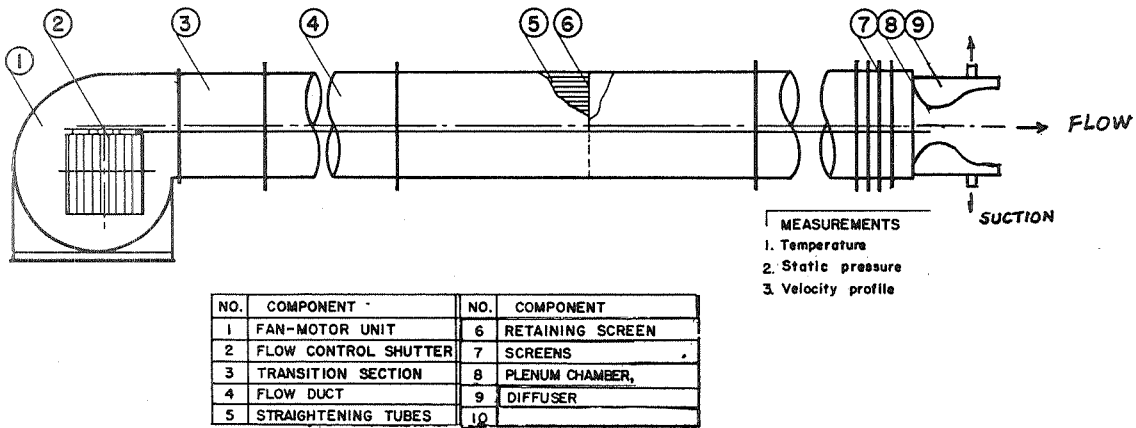
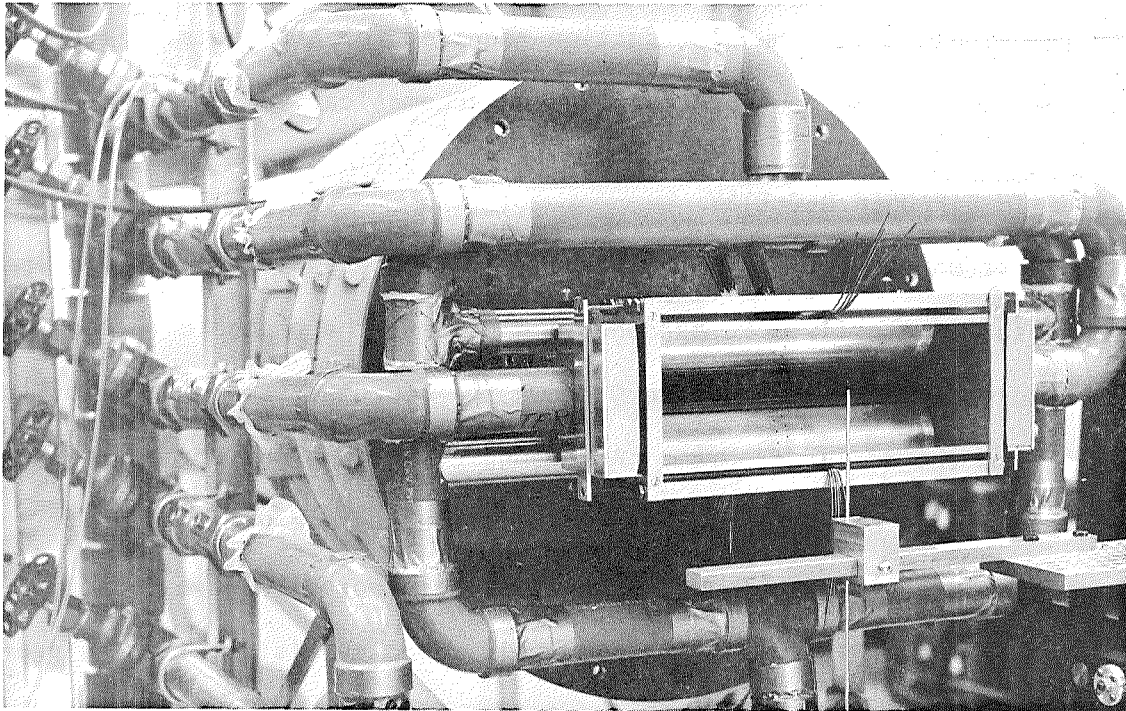
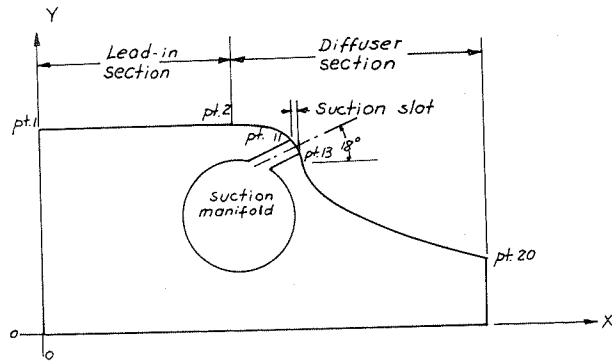


Figure 8. Test arrangement shown pictorially and schematically.



pt.	X(in.)	X(cm)	Y(in.)	Y(cm)
1	0.000	0.000	2.250	5.715
2	1.800	4.572	2.250	5.715
3	2.000	5.080	2.244	5.700
4	2.100	5.334	2.239	5.685
5	2.200	5.588	2.227	5.657
6	2.300	5.842	2.213	5.621
7	2.400	6.096	2.194	5.573
8	2.500	6.350	2.168	5.507
9	2.600	6.604	2.129	5.408
10	2.700	6.858	2.065	5.245
11	2.760	7.010	1.965	4.991
12	2.800	7.112	1.917	4.869
13	2.840	7.214	1.767	4.488
14	2.900	7.366	1.633	4.148
15	3.100	7.874	1.445	3.670
16	3.400	8.636	1.265	3.213
17	3.800	9.652	1.090	2.749
18	4.200	10.668	0.959	2.436
19	4.600	11.684	0.853	2.167
20	4.900	12.446	0.779	1.979

Figure 9. Griffith diffuser geometry with coordinates obtained from design program.

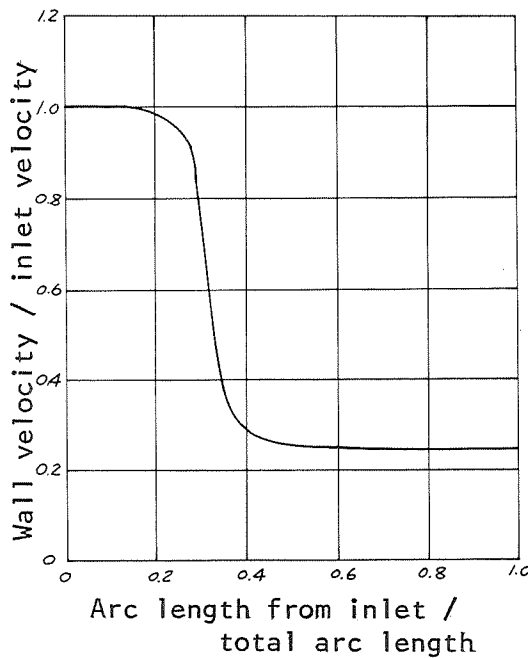


Figure 10. Wall velocity distribution prescribed to diffuser design program. AR = 4.

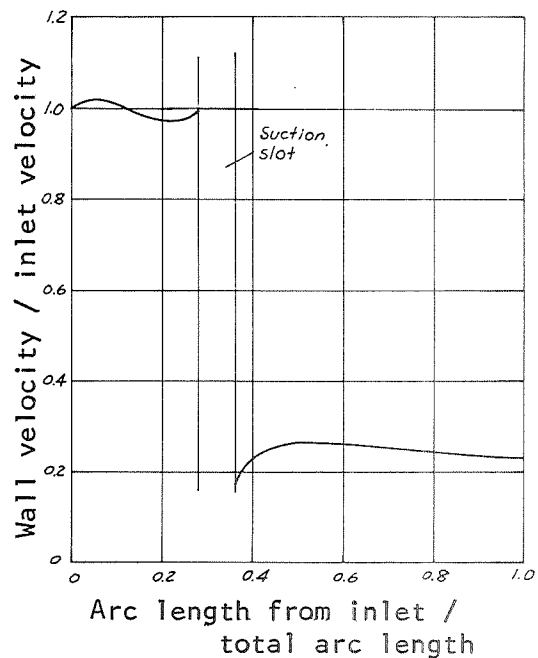
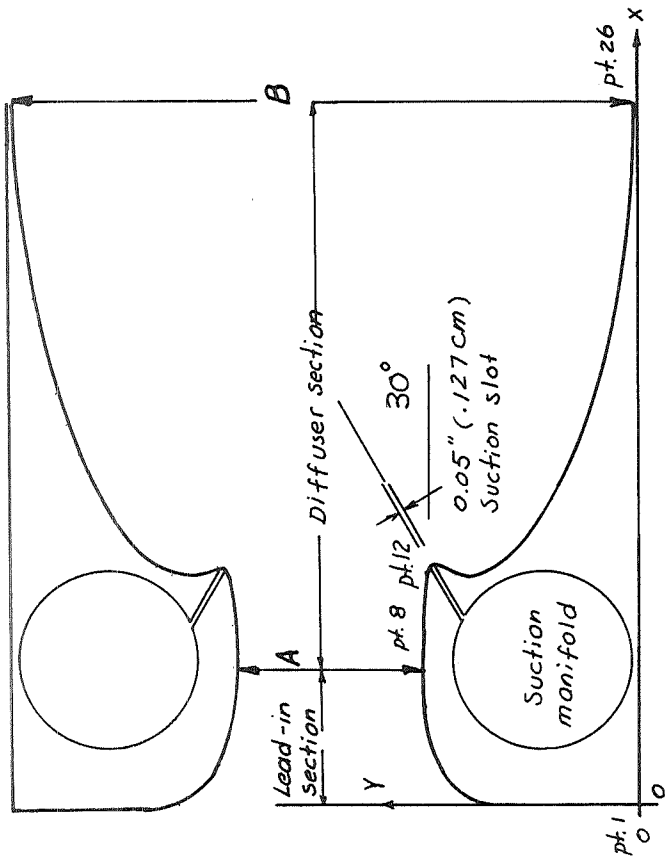


Figure 11. Wall velocity distribution predicted by computer analysis program when 10% suction rate is applied.

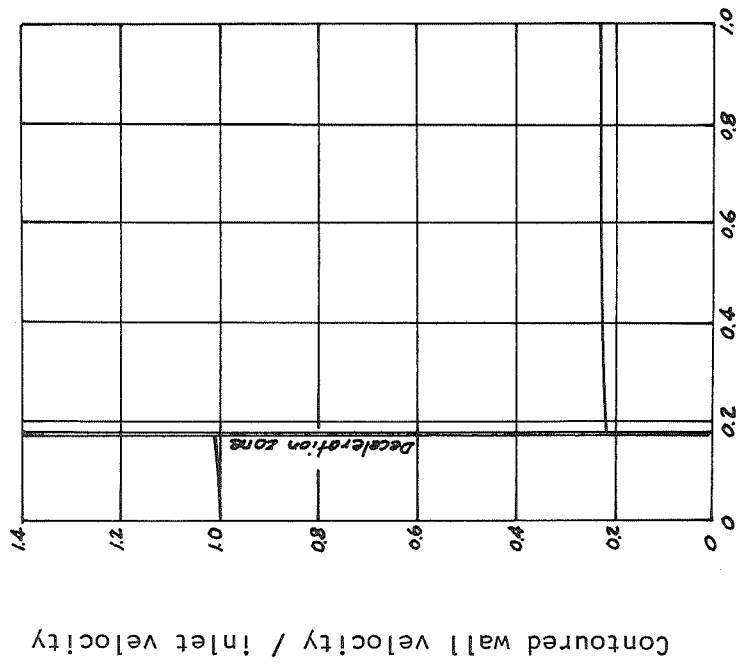


AR	A (in.)	B (in.)	A (cm)	B (cm)
2	2.0	6.0	7.62	15.24
3	1.5	4.5	3.81	11.43
4	1.0	4.0	2.54	10.16

Figure 12. Griffith diffuser geometry with coordinates obtained from design program.

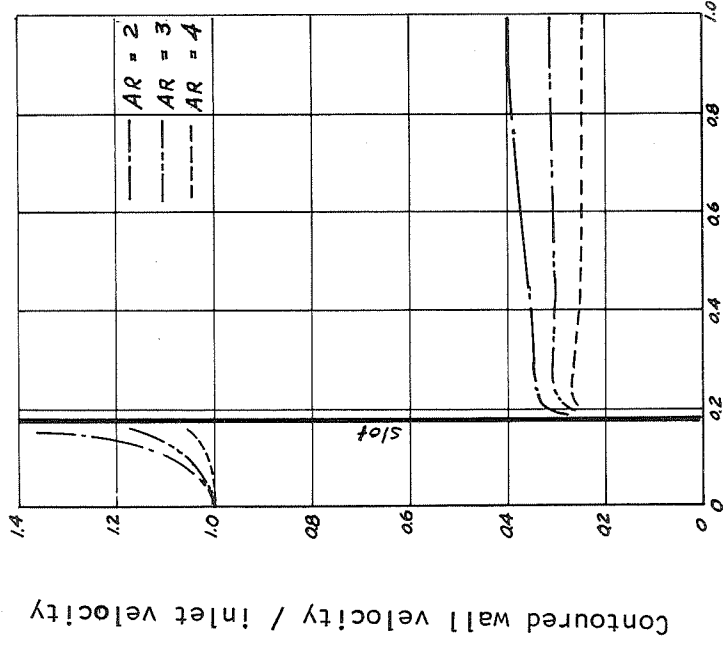
pt.	X (in.)	Y (in.)	pt.	X (in.)	Y (in.)
1	0	2.000	14	1.653	3.210
2	0	3.100	15	1.644	3.190
3	0.149	3.308	16	1.637	3.164
4	0.315	3.391	17	1.667	3.026
5	0.535	3.443	18	1.770	2.858
6	0.714	3.463	19	1.958	2.677
7	0.849	3.470	20	2.231	2.504
8	0.939	3.471	21	2.525	2.374
9	1.119	3.467	22	2.889	2.260
10	1.401	3.437	23	3.381	2.156
11	1.603	3.386	24	3.995	2.076
12	1.677	3.296	25	4.603	2.024
13	1.660	3.244	26	4.904	2.003

pt.	X (cm)	Y (cm)	pt.	X (cm)	Y (cm)
1	0	5.080	14	4.199	8.153
2	0	7.874	15	4.176	8.103
3	0.378	8.402	16	4.158	8.037
4	0.800	8.613	17	4.234	7.686
5	1.359	8.745	18	4.496	7.259
6	1.814	8.796	19	4.973	6.800
7	2.156	8.814	20	5.667	6.360
8	2.385	8.816	21	6.414	6.030
9	2.842	8.806	22	7.338	5.740
10	3.559	8.790	23	8.588	5.476
11	4.072	8.600	24	10.147	5.273
12	4.260	8.372	25	11.692	5.141
13	4.216	8.240	26	12.456	5.088



Arc length from inlet / total arc length

Figure 13. Wall velocity distribution prescribed to diffuser design program. AR = 4.



Arc length from inlet / total arc length

Figure 14. Wall velocity distribution predicted by computer analysis program with suction slot added.

predicted velocities are indicated for a suction rate of 10% through a slot added at the deceleration zone.

4.3 CIRCULAR ARC DIFFUSER GEOMETRY

The best performing circular arc diffuser as determined from preliminary tests had an area ratio of 2 1/2 to 1 and a slot located at 15° measured from the inlet junction. Figure 15 shows a typical assembled circular arc diffuser, which consisted of four components: the inlet section, the cradle, the circular arc walls, and the exit section. The inlet section consisted of two parallel plates. They were inserted in the cradle at a fixed distance apart so that the flow entered the divergent channel tangentially. The edges of the parallel plates were made knife-sharp to minimize the "step effect" at the inlet junction. The cradle acted as a frame to hold the inlet section, the diffuser walls, and the exit section at specified relative positions. The circular arc diffuser walls consisted of two half-cylinders mounted on a pair of tubes. The tubes were rested on the bearing surfaces of the cradle. Each half-cylinder could be rotated within the bearing surfaces to adjust the slot position. The exit section also consisted of two plates, each having a sharp edge to minimize the "step effect" at the exit junction. The spacing between the parallel plates of the exit section could be adjusted so as to vary the exit area to inlet area ratio between the limits of 1 to 1 and 4 to 1. Figure 16 shows the circular wall detail. Four pairs of half-cylinders of the same overall dimensions but with different slot geometries were designed to examine the effect of slot geometry on the performance of the circular arc diffuser. Figures 17-a, b, c, and d show the various slot geometries used. The

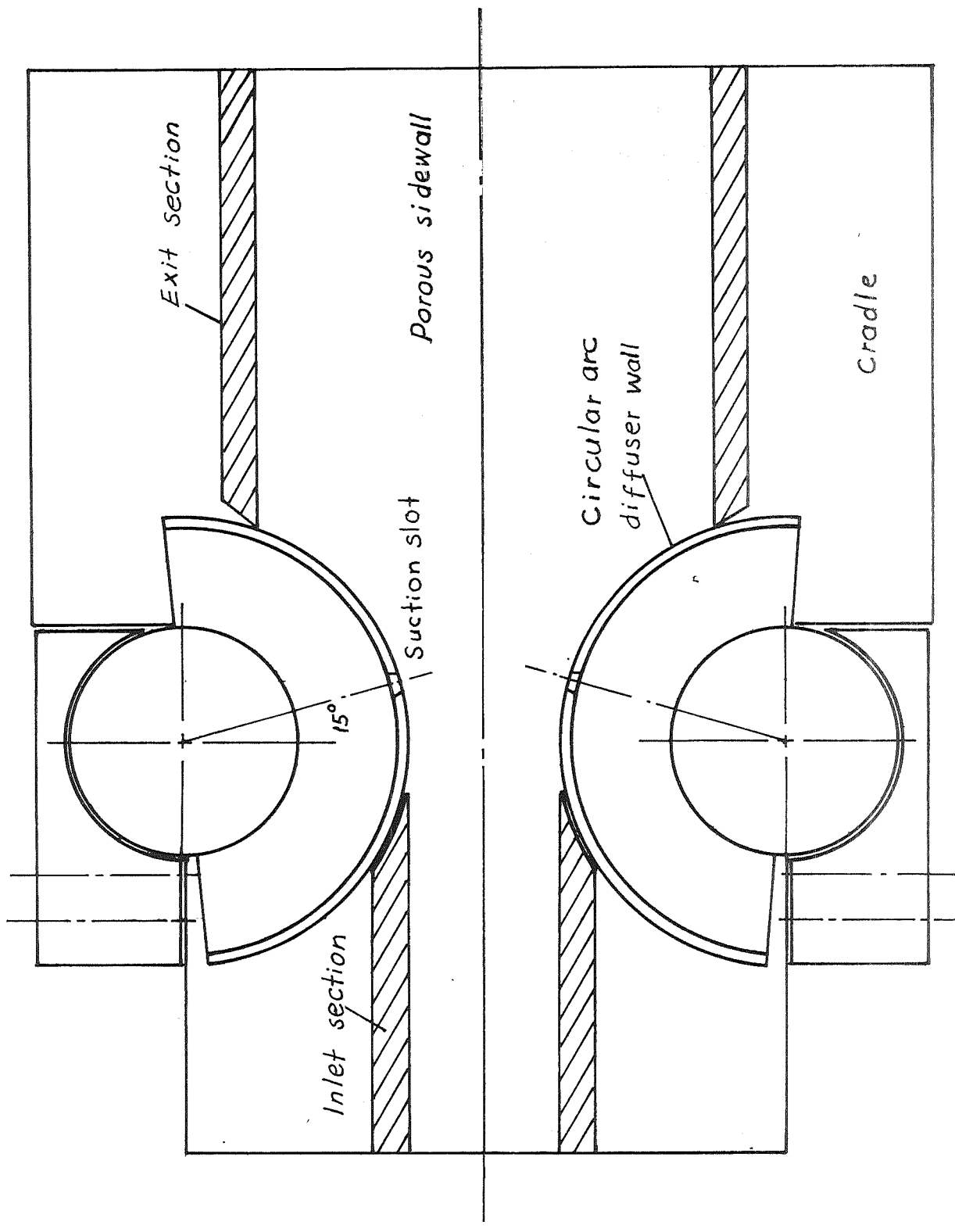


Figure 15. Typical assembled circular-arc diffuser.

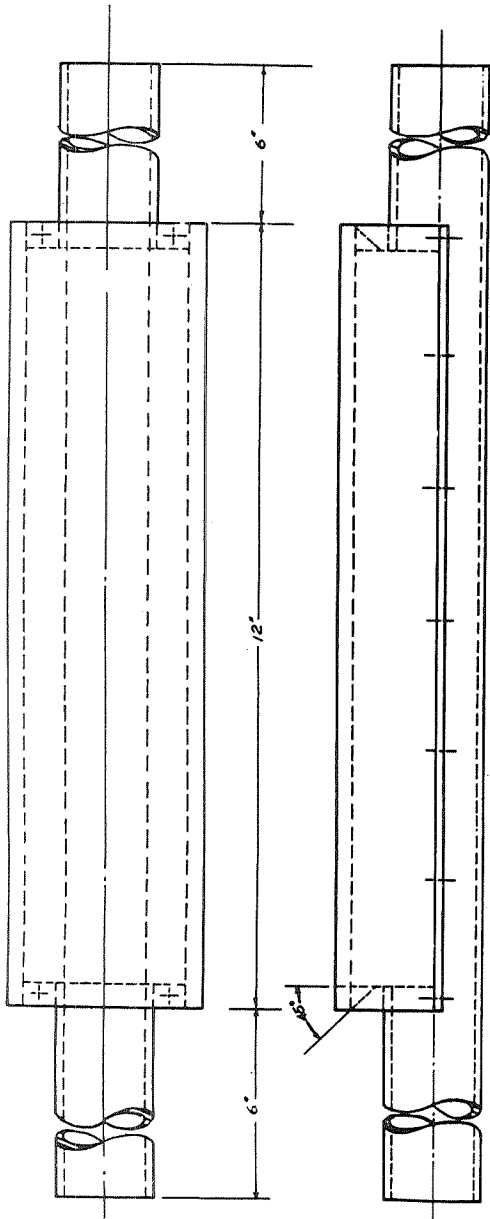


Figure 16. Circular arc diffuser wall.

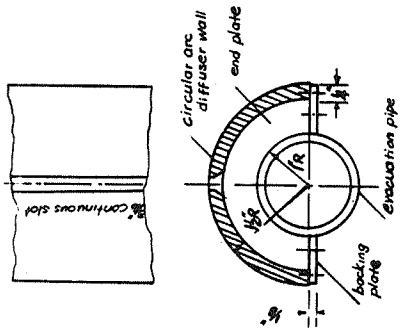


Figure 17-a
3/16" Continuous slot.

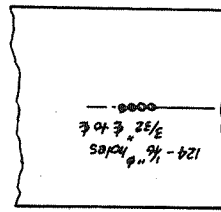


Figure 17-b
1/16" Continuous slot.

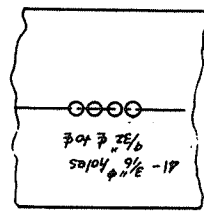


Figure 17-c
3/16" Suction holes.

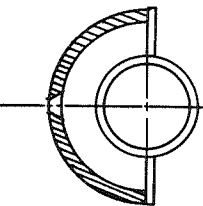


Figure 17-d
1/16" Suction holes.

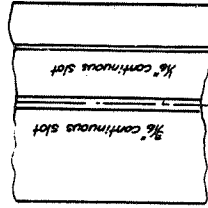
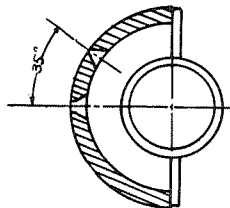


Figure 17-e
Double suction slots.



double-slot design is shown in Figure 17-e. This design utilized the already existing 3/16 inch (0.476 cm) single-slot configuration. A 1/16 inch (0.159 cm) slot was added 35° from the 3/16 inch (0.476 cm) slot. Since an existing configuration was utilized, independent control of the suction rate through each of the two slots could not be implemented. The positions of the two slots relative to each other could not be changed, although this would have been desirable. This design was tested at an area ratio of 4 to 1.

4.4 INSTRUMENTATION AND MEASUREMENTS

The stagnation pressure at the end of the duct and the static pressure at the diffuser inlet were measured with a micromanometer having resolution of 0.001 inch of water. Nine pressure taps were installed in each circular arc diffuser wall, and fourteen taps were installed in each Griffith diffuser wall. The wall pressure distribution (including the static pressure at the diffuser inlet) was measured by using a flush mounted pressure transducer of range 0-1.0 psid, and a rapid scanning mechanism with a capacity of 48 channels. The output of the transducer was automatically recorded on paper tape for subsequent analysis. The scanning rate was set at 24 channels per second and hence a set of pressure distribution measurements could be completed in two seconds.

The velocity distribution at various planes normal to the centerline of the test section were measured with miniature constant temperature hot-wire probes. Each probe was calibrated by placing it near a pitot-static probe in a standard flow nozzle, varying the air velocity from approximately 20 to 250 ft./sec., and recording simultaneous voltage and manometer

readings. The voltage output of the hot-wire probe was displayed by a multi-range digital voltmeter with a selective damping device. The probe was positioned with a traversing mechanism adapted from a milling machine bed. It had a position resolution of 0.001 inch (0.0025 cm) in each of the three directions. For the circular arc diffusers, velocity profiles were normally obtained in X-Y planes located at Z = 0.5, 1.0, 2.0, 3.0, and 4.5 (diffuser heights downstream from entrance. See Figure 18.). For the Griffith diffusers, velocity profiles were obtained in the exit plane and in a plane approximately halfway between inlet and exit. At the diffuser inlet, the velocity was measured only at the center of the flow channel.

In obtaining the horizontal velocity profiles, approximately 14 velocity measurements were made along the sidewall-to-sidewall horizontal centerline in each of the X-Y planes named above. From 5 to 20 velocity measurements, depending upon the local diffuser height, were made along the vertical centerline to obtain the vertical velocity profile. These velocities were normalized to the maximum velocity throughout the local X-Y plane.

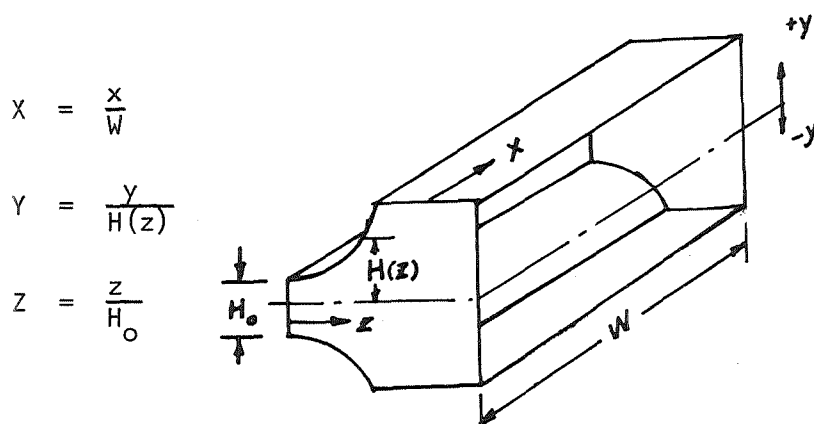


Figure 18. Nomenclature for velocity measurements.

Calibrated laminar flow tubes were used to measure the slot and side-wall suction flow rates. Independent control and measuring of the suction rate through each sidewall, the top wall slot, and the bottom wall slot was achieved by individual hand valves.

A copper-constantan thermocouple was used to measure the air temperature, and a well-type mercury barometer was used to obtain atmospheric pressure.

A volume flow balance was made for several runs. For the circular arc diffusers, velocities were measured at 36 locations (see Figure 19) in each of three planes: $Z = 2.0, 3.0$ and 4.5 . The resulting flow rates were compared with the inlet flow rates determined by the dynamic pressure. For the Griffith diffusers, the exit volume flow rate was obtained from velocity measurements at 91 stations in the exit plane (similar to Figure 19 except that 7 rows and 13 columns were used).

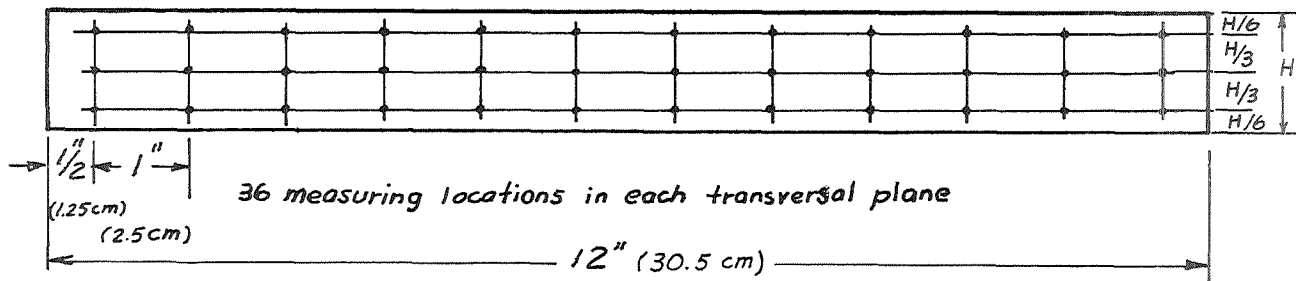


Figure 19. Locations for velocity measurement in making volume flow rate balances on circular arc diffusers.

SECTION V
TEST CONDITIONS AND PROCEDURE

5.1 TEST CONDITIONS

It was originally planned to run all diffuser tests (except those made to determine a transition Reynolds number) with an inlet velocity of 250 ft/sec (76.2 m/sec). However, preliminary test runs indicated that for the Griffith diffuser tests a lower inlet velocity was necessary. The inlet velocity for the Griffith diffuser tests was limited to about 50 ft/sec (15.2 m/sec) because the capacity of the suction blower was inadequate to handle the very high suction rates needed for higher inlet velocities. The following is a summary of the test conditions used for the Griffith diffuser tests:

Inlet air velocity - 50 ft/sec (15.2 m/sec).

Area ratios - 2, 3, and 4.

Corresponding inlet Reynolds numbers - 115,000; 65,000; 45,000.

Corresponding inlet volume flow rates - 12.5 CFS ($0.354 \text{ m}^3/\text{sec}$);

6.25 CFS ($0.177 \text{ m}^3/\text{sec}$); 3.125 CFS ($0.0885 \text{ m}^3/\text{sec}$)

Suction slot - 0.05 inch (0.127 cm) continuous slot.

Total slot suction rates - ranged from 0% to 45% of the inlet flow rates.

Total sidewall suction rates - ranged from 10% to 20% of the inlet flow rates.

As listed in the Appendix, 34 preliminary tests were made on the circular arc diffuser having one slot per wall. The primary objective of these preliminary runs was to establish the best slot location and the

highest area ratio resulting in a stable distributed flow at the exit plane, yet meeting a slot suction limit of 10%. These preliminary tests indicated that an area ratio of 2.5 and a slot located 15° from the diffuser entrance was optimum. The subsequent tests on the circular arc diffusers having one slot per wall were made with the following test conditions:

Inlet air velocity - 250 ft/sec (76.2 m/sec).

Area ratio - 2.5.

Inlet Reynolds number - 230,000.

Inlet volume flow rate - 20.8 CFS ($0.590 \text{ m}^3/\text{sec}$).

Slot geometries - $3/16$ inch (0.476 cm) continuous slot; $1/16$ inch (0.159 cm) continuous slot; $3/16$ inch (0.476 cm) diameter holes with center-to-center spacing of 1.5 diameters; $1/16$ inch (0.159 cm) diameter holes with center-to-center spacing of 1.5 diameters.

Slot location - 15° from diffuser entrance.

Total slot suction - from 0% to 10% of inlet flow.

Total sidewall suction - near 3.5% of inlet flow.

For the circular arc diffuser having two slots per wall, the following test conditions were used:

Inlet air velocity - 250 ft/sec (76.2 m/sec).

Area ratio - 4.

Inlet Reynolds number - 230,000.

Inlet volume flow rate - 20.8 CFS ($0.590 \text{ m}^3/\text{sec}$).

Slot geometry - a $3/16$ inch (0.476 cm) continuous slot at 15° and a $1/16$ inch (0.159 cm) continuous slot at 50° from entrance.

Total slot suction - from 0% to 10% of inlet flow.

Total sidewall suction - near 4% of inlet flow.

For all diffuser tests, air was delivered by the fan from the test room through the diffuser, and the diffuser discharged the air back into the test room.

5.2 TEST PROCEDURE

The same test procedure was used for both Griffith and circular arc diffusers. The diffuser test section was attached to the end of the main air duct. The air delivery fan and the suction blower were started. The fan inlet shutter was adjusted to give the desired inlet air velocity as measured by the static pressure differential between the diffuser inlet and the main duct.

After steady state was established, three independent pressure measurements were made with the micromanometer: (1) the static pressure at the diffuser inlet, (2) the static pressure at the end of the air duct, (3) the pressure differential between (1) and (2).

The sidewall and the slot suction rates were initially set higher than the specified values and then gradually reduced to the desired values by manipulating the appropriate hand valves. The left and right sidewall suction rates were adjusted to be equal as were the top and bottom slot suction rates.

The curved wall static pressure readings were obtained by using the pressure transducer in conjunction with the scanning valve, and these readings were recorded on paper tape. Three sets of values were recorded at the beginning of each test. Thermocouple and barometer readings were made during the test.

The reference position of the hot-wire probe traversing mechanism was examined prior to making velocity measurements. Velocity measurements were then made at the various stations using the traversing mechanism to position the probe. If the hot-wire filament was damaged during a test run, a new probe was calibrated and the test run repeated. In all velocity measurements, a record was kept to identify the individual probe with its calibration curve.

Near the end of the run, three additional sets of wall static pressure readings were made.

The measurements taken were used to obtain the following information for each diffuser test run:

- (1) Diffuser effectiveness, η , where

$$\eta = \frac{P_{s,e} - P_{s,i}}{P_{d,i} \left[1.0 - \left(\frac{1.0 - \% \text{ total suction}}{AR} \right)^2 \right]}$$

Although this equation accounts for the effect of suction upon the exit velocity, it does not penalize the diffuser for the energy associated with the removal of the suction air.

- (2) Inlet Reynolds number:

$$\text{Re No.} = \left[\frac{(4 A_{cs} / \text{perimeter}) (\text{velocity})}{\text{fluid kinematic viscosity}} \right]_{\text{diffuser inlet}}$$

(3) Total pressure loss as computed from the diffuser effectiveness:

$$\text{Total pressure loss} = (1.0 - \eta) \left[1.0 - \left(\frac{1.0 - \% \text{ total suction}}{AR} \right)^2 \right] \left(\frac{\rho V^2}{2g_c} \right)_i$$

where $\left(\frac{\rho V^2}{2g_c} \right)_i$ is the inlet dynamic pressure.

The pressure losses were reported as a percentage of inlet total pressure and inlet dynamic pressure.

(4) Total slot suction rate as a percentage of inlet flow.

(5) Total sidewall suction rate as a percentage of inlet flow.

(6) Horizontal velocity distributions at various planes downstream from the diffuser entrance.

(7) Vertical velocity distributions at various planes downstream from the diffuser entrance.

(8) Wall pressure coefficient distributions along the top and bottom contoured diffuser walls. The pressure coefficient was obtained from the equation:

$$C_p = \frac{V_i^2 - V_z^2}{V_i^2}$$

and the velocities were obtained from wall pressure readings.

(9) Centerline velocity distribution from diffuser entrance to diffuser exit.

(10) Comparison of items (8) and (9) with predicted values from computer analyses.

SECTION VI

DISCUSSION OF RESULTS

6.1 GRIFFITH DIFFUSER (FIRST DESIGN)

As mentioned in paragraph 4.2, the first of the two Griffith diffusers could not be operated without separation occurring before the suction slot unless extremely high suction rates were applied. Approximately 75% of the inlet flow rate had to be removed by suction in order to prevent separation. Several modifications to the slot geometry were made in attempts to yield satisfactory operation, but none was successful. It is believed that the reason for the failure of this diffuser to perform satisfactorily is as follows. In the early period of the investigation it was thought that the sink effect of slot suction could be utilized advantageously so as to decrease the required deceleration within the region of the slot. Some deceleration was prescribed to occur both upstream and downstream of the slot as shown in Figure 10. The slot suction was to have a sink effect on the flow to compensate for the deceleration. Apparently the suction was not capable of exerting an adequate influence on the potential core sufficiently beyond the slot to achieve the desired results.

No detailed test runs were made on this diffuser. The results would have little meaning because with flow separation occurring upstream of the slot, diffuser performance is poor and no correlation between measured and computed velocities and pressures could be expected.

6.2 GRIFFITH DIFFUSER (SECOND DESIGN)

With the failure of the first Griffith diffuser to perform satisfactorily, the design philosophy was changed so as to prescribe a small

acceleration from the diffuser entrance to the slot and from the slot to the diffuser exit as shown earlier in Figure 13.

Figures 20 and 21 show the wall pressure and the velocity distributions for the second Griffith diffuser when operated with an area ratio of 2. Figure 20 shows good correlation between the measured wall pressures and centerline velocities and those predicted by the computer analysis program. The uniform velocity distribution at the exit plane as shown in Figure 21 and the diffuser effectiveness of 99% are especially significant in view of the desirable characteristics listed in the Introduction. The diffuser total pressure loss was only 8.4×10^{-5} psia (0.0044 mm Hg), which was 0.44% of the inlet dynamic pressure or 0.0006% of the inlet total pressure.

However the desirable results were achieved by applying about four times the slot suction rate indicated to be necessary by Taylor's criterion. When operating with an area ratio of 2.0, approximately 16% of the inlet flow had to be removed through the slot for a completely stable distributed flow. It was possible to reduce the suction rate to a minimum of approximately 11% without separation provided no disturbances in the flow occurred. If flow separation occurred, the suction rate had to be increased to 16% to restore the unseparated flow pattern.

Figures 22 and 23 show the wall pressure and the velocity distributions with the slot suction rate decreased to 11%. Although the results are essentially the same as when operated with a suction rate of 16%, only quasi-stable performance was possible.

Figures 24 and 25 show the pressure and velocity distributions when no slot suction is applied. The horizontal velocity distribution indicates that the sidewall suction was sufficient to cause essentially two-dimensional

Run no. 1 0.05 in (0.127 cm) slot Area ratio = 2.0 $V_{inlet} = 48.5 \text{ ft/sec (14.8 m/sec)}$
 $\eta = 99.5\%$ Slot suction = 16.2% S.W. suction = 11.6% Reynolds number = 115,000
 $P_{loss} = 0.0006\%$ $P_{t,i} = 14.602 \text{ psia (755 mm Hg)}$ $P_{s,i} = 14.583 \text{ psia (754 mm Hg)}$ $P_{s,e} = P_{atm} = 14.600 \text{ psia (755 mm Hg)}$

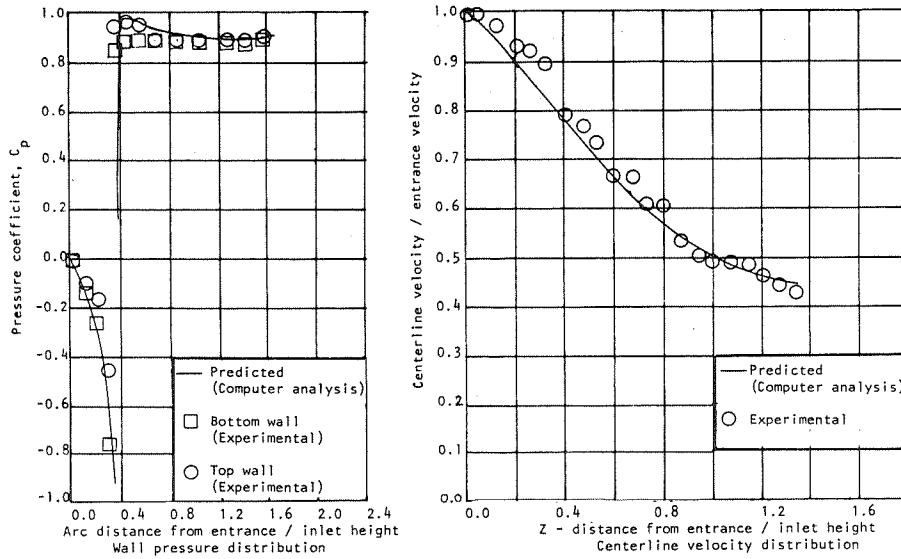


Figure 20. Wall pressure and centerline velocity distribution for Griffith diffuser.

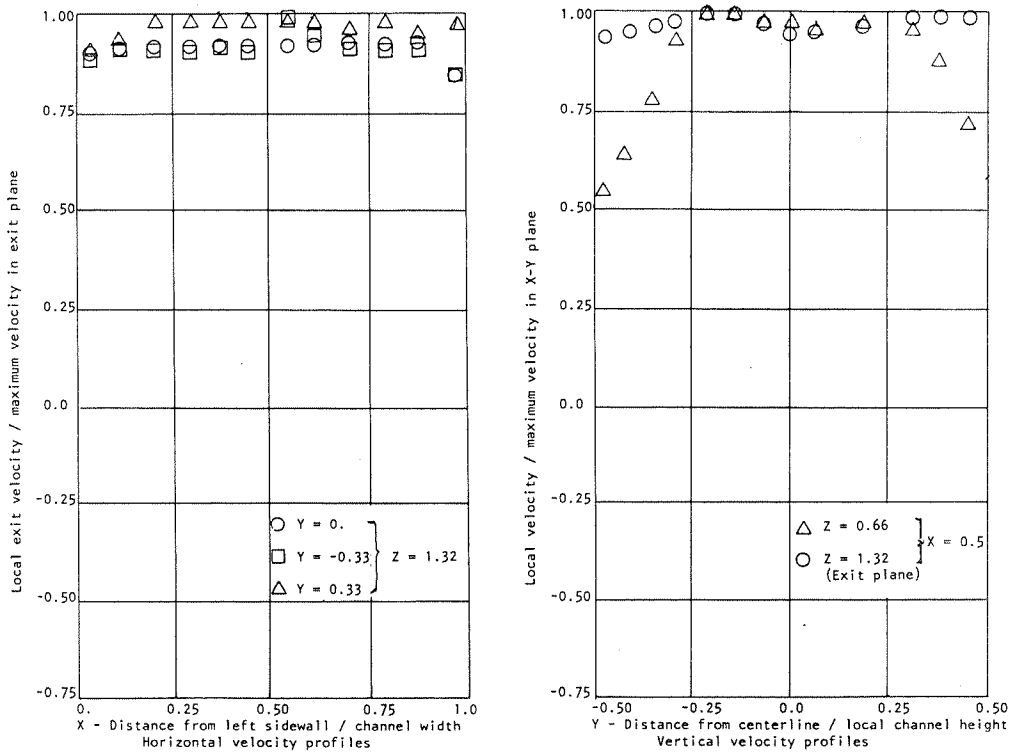


Figure 21. Velocity profiles for Griffith diffuser.

Run no. 2 0.05 in (0.127 cm) slot Area ratio = 2.0 $V_{inlet} = 49 \text{ ft/sec (15 m/sec)}$
 $\eta = 98.8\%$ Slot suction = 11.7% S.W. suction = 11.6% Reynolds number = 115,000
 $P_{loss} = 0.0014\%$ $P_{t,i} = 14.603 \text{ psia (755 mm Hg)}$ $P_{s,i} = 14.584 \text{ psia (754 mm Hg)}$ $P_{s,e} = P_a = 14.600 \text{ psia (755 mm Hg)}$

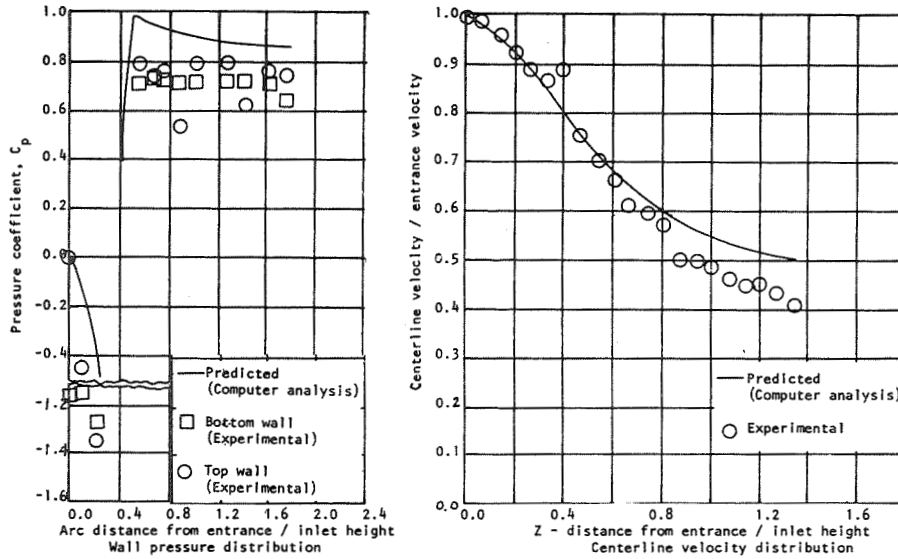


Figure 22. Wall pressure and centerline velocity distribution for Griffith diffuser.

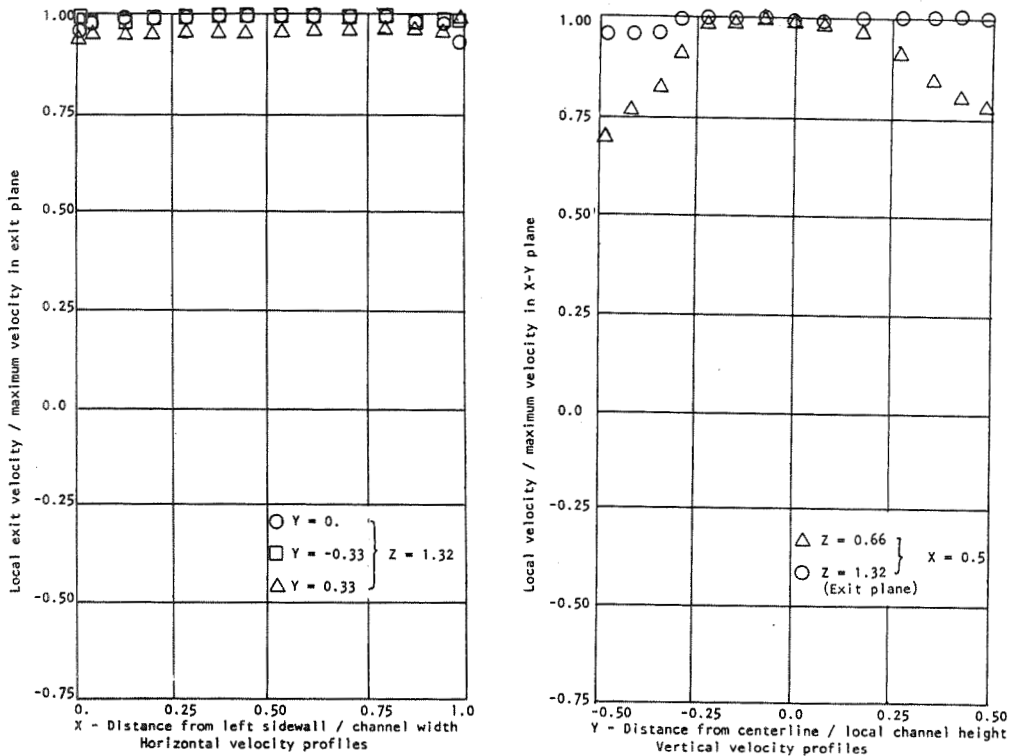


Figure 23. Velocity profiles for Griffith diffuser.

Run no. 3 0.05 in (0.127 cm) slot Area ratio = 2.0 $V_{inlet} = 45.5$ ft/sec (14 m/sec)
 $n = 37.0\%$ Slot suction = 0.0% S.W. suction = 11.6% Reynolds number = 108,000
 $P_{loss} = 0.057\%$ $P_{t,i} = 14.611$ psia (756 mm Hg) $P_{s,i} = 14.595$ psia (755 mm Hg) $P_{s,e} = P_a = 14.600$ psia (755 mm Hg)

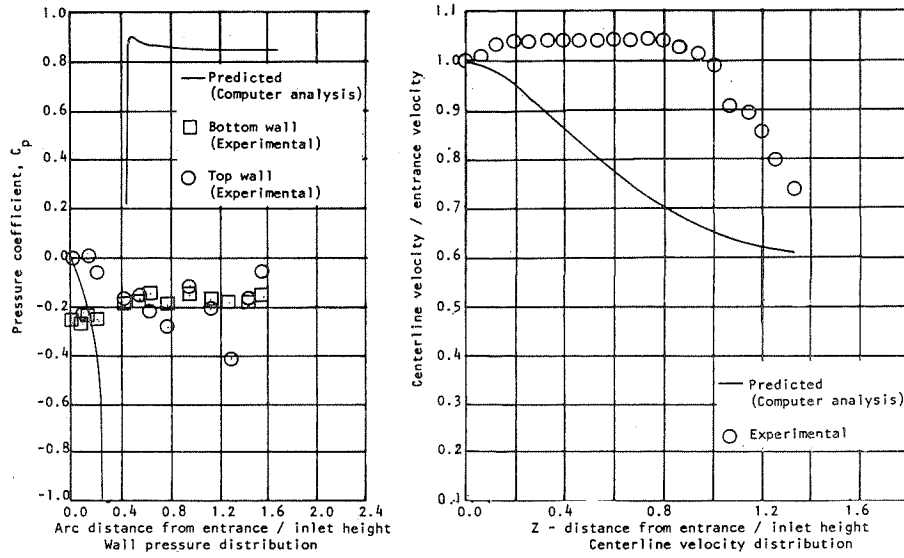


Figure 24. Wall pressure and centerline velocity distribution for Griffith diffuser.

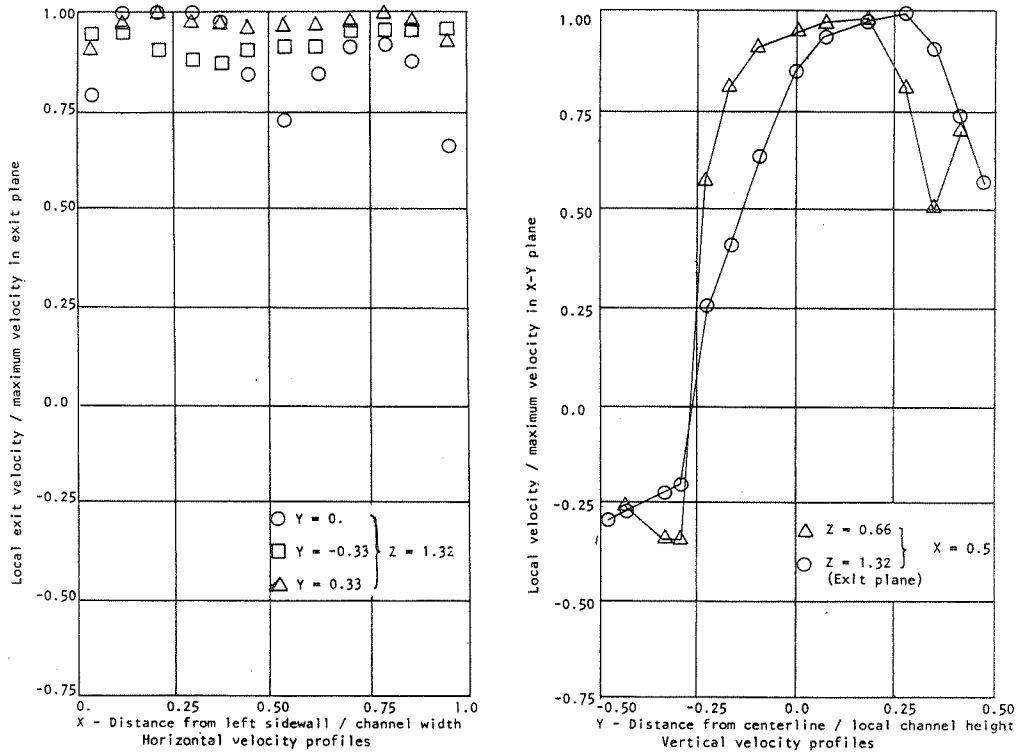


Figure 25. Velocity profiles for Griffith diffuser.

flow. The vertical velocity distribution was very poor as expected. A slight preference for the top wall is observed with severe flow separation and reversal occurring at the bottom wall.

Figures 26 and 27 show the pressure and velocity distributions for the same diffuser when operated with an area ratio of 3. In order to achieve completely stable distributed flow, the suction rate had to be increased to 36.3%. The required suction rate for unseparated flow with operation at an area ratio of 3.0 had to be significantly higher than with operation at an area ratio of 2.0. The diffuser inlet height was only one-half as large when operating with an area ratio of 3.0 as compared with operation at an area ratio of 2.0. If the same amount of fluid had to be removed in the two cases, the percentage suction would thus be twice as large for operation with an area ratio of 3.0. Actually, somewhat more fluid had to be removed with operation at an area ratio of 3.0, as predicted by Taylor's criterion (discussed in paragraph 3.2). Consequently, somewhat more than twice the suction rate was required.

Quasi-stable operation was possible with a slot suction rate as low as 22% when operating with an area ratio of 3.0. Again, unseparated flow was possible provided no flow disturbance occurred. An increase of suction rate to 36% was necessary to restore unseparated flow if a flow disturbance caused separation to occur. Figures 28 and 29 show the pressure and velocity distributions with a slot suction rate of 22% and an area ratio of 3.0. They are very similar to Figures 26 and 27, and the diffuser effectiveness remains at just under 98%.

Figures 30 and 31 show the pressure and velocity distributions when operating with an area ratio of 3.0 and with no slot suction. Since

Run no. 4 0.05 in (0.127 cm) slot Area ratio = 3.0 $V_{inlet} = 50 \text{ ft/sec (15.2 m/sec)}$
 $\eta = 97.8\%$ Slot suction = 36.3% S.W. suction = 18.0% Reynolds number = 66,000
 $P_{loss} = 0.0029\%$ $P_{t,i} = 14.601 \text{ psia (755 mm Hg)}$ $P_{s,i} = 14.581 \text{ psia (754 mm Hg)}$ $P_{s,e} = P_a = 14.600 \text{ psia (755 mm Hg)}$

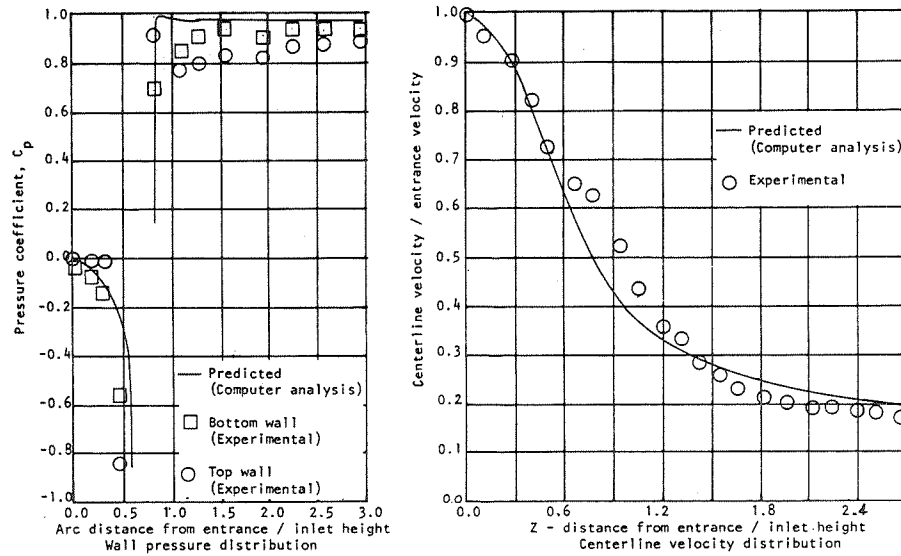


Figure 26. Wall pressure and centerline velocity distribution for Griffith diffuser.

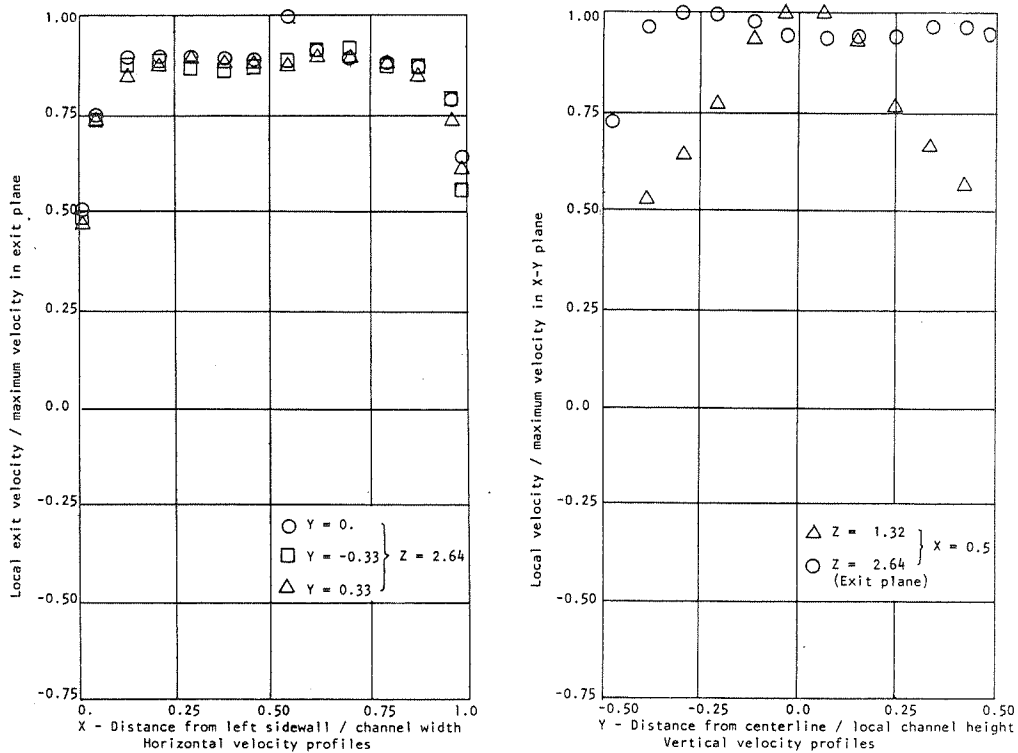


Figure 27. Velocity profiles for Griffith diffuser.

Run no. 5 0.05 in (0.127 cm) slot Area ratio = 3.0 $V_{inlet} = 50 \text{ ft/sec (15.2 m/sec)}$
 $n = 97.8\%$ Slot suction = 21.6% S.W. suction = 14.5% Reynolds number = 66,000
 $P_{loss} = 0.0029\%$ $P_{t,i} = 14.601 \text{ psia (755 mm Hg)}$ $P_{s,i} = 14.581 \text{ psia (754 mm Hg)}$ $P_{s,e} = P_a = 14.600 \text{ psia (755 mm Hg)}$

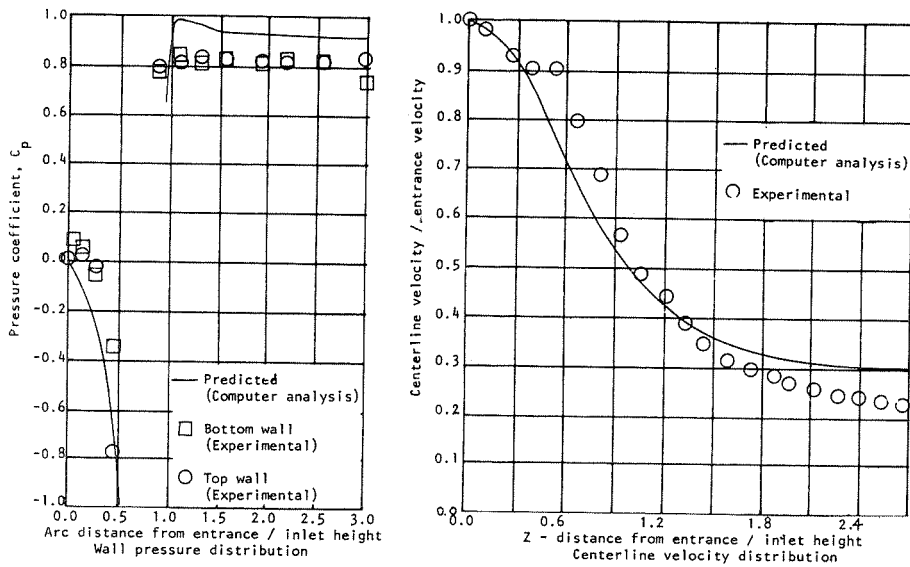


Figure 28. Wall pressure and centerline velocity distribution for Griffith diffuser.

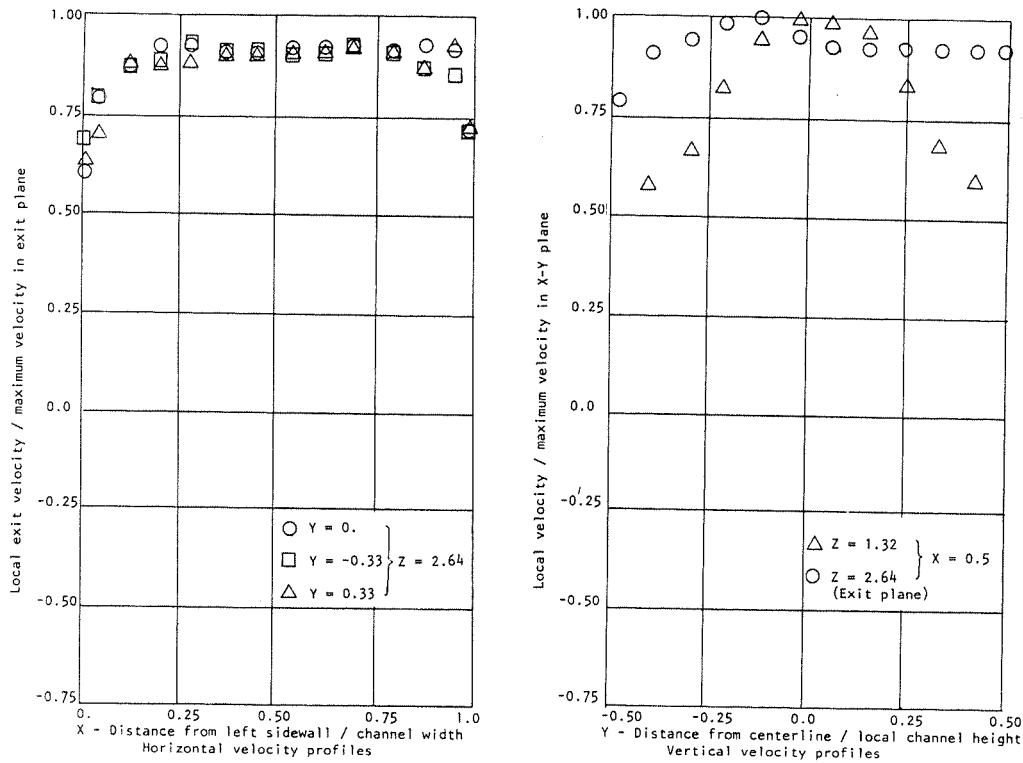


Figure 29. Velocity profiles for Griffith diffuser.

Run no. 6 0.05 in (0.127 cm) slot Area ratio = 3.0 $V_{inlet} = 48$ ft/sec (15 m/sec)
 $\eta = 18.3\%$ Slot suction = 0.0% S.W. suction = 18.7% Reynolds number = 64,000
 $P_{loss} = 0.094\%$ $P_{t,i} = 14.615$ psia (756 mm Hg) $P_{s,i} = 14.597$ psia (755 mm Hg) $P_{s,e} = P_a = 14.600$ psia (755 mm Hg)

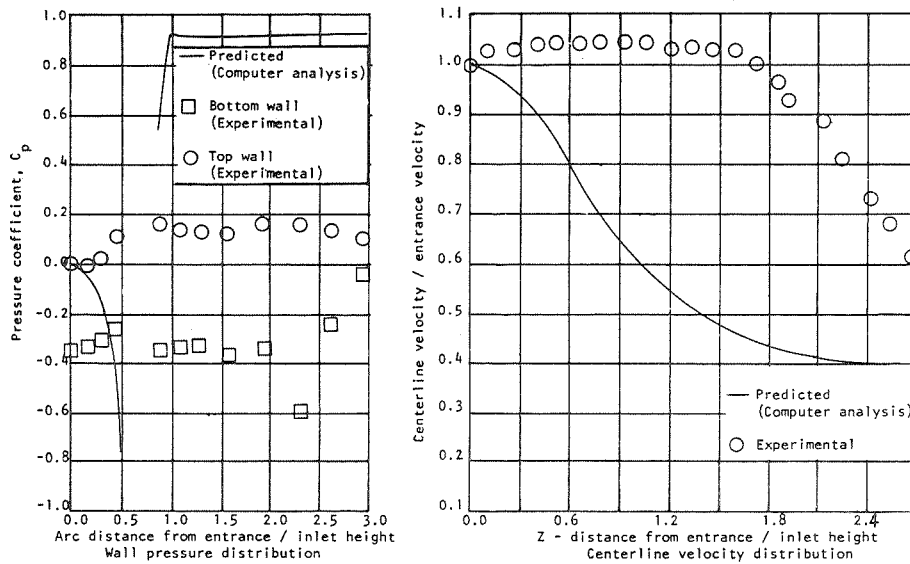


Figure 30. Wall pressure and centerline velocity distribution for Griffith diffuser.

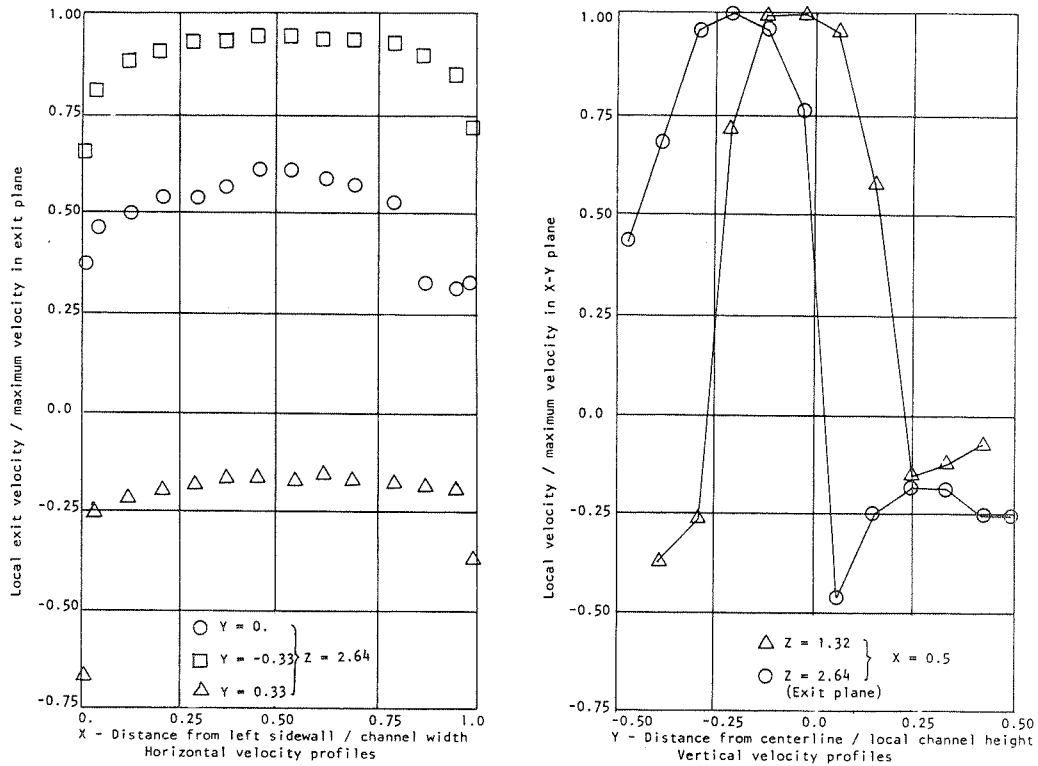


Figure 31. Velocity profiles for Griffith diffuser.

early separation occurs, no correlation exists between experimental values and predicted values of wall pressure and centerline velocity distributions. Diffuser effectiveness dropped to about 18%. Table 1 summarizes the results of the tests made on the second Griffith diffuser as discussed in the preceding paragraphs. Data were also taken with a 4 to 1 area ratio but no detailed plots were made because of flow separation at reasonable suction rates.

TABLE 1. GRIFFITH DIFFUSER TEST RESULTS

Test No.	Slot Geometry	Area Ratio	Inlet Velocity		Inlet Reynolds Number	% Suction	
			Ft/sec	M/sec		Slots	Sidewalls
1	0.05 in (0.127 cm) continuous	2.0	48.5	14.8	115,000	16.2	11.6
2	0.05 in (0.127 cm) continuous	2.0	49.0	15.0	115,000	11.7	11.6
3	0.05 in (0.127 cm) continuous	2.0	45.5	14.0	108,000	0.0	11.6
4	0.05 in (0.127 cm) continuous	3.0	50.0	15.2	66,000	36.3	18.0
5	0.05 in (0.127 cm) continuous	3.0	50.0	15.2	66,000	21.6	14.5
6	0.05 in (0.127 cm) continuous	3.0	48.0	14.6	64,000	0.0	18.7

Test No.	Total Inlet Pressure		$(\Delta P)_{\text{static}}$ $P_{s,e} - P_{s,i}$		Total Pressure Loss		Effectiveness η %
	Psia	mm Hg	Psi	mm Hg	% of Inlet Dynamic	Total	
1	14.602	755	0.017	0.86	0.44	0.0006	99.5
2	14.603	755	0.016	0.84	1.03	0.0014	98.8
3	14.611	756	0.005	0.26	51.00	0.0570	37.0
4	14.601	755	0.019	0.97	2.15	0.0029	97.8
5	14.601	755	0.019	0.97	2.11	0.0029	97.8
6	14.615	756	0.003	0.16	75.80	0.0940	18.3

Contours of constant velocity / average velocity.

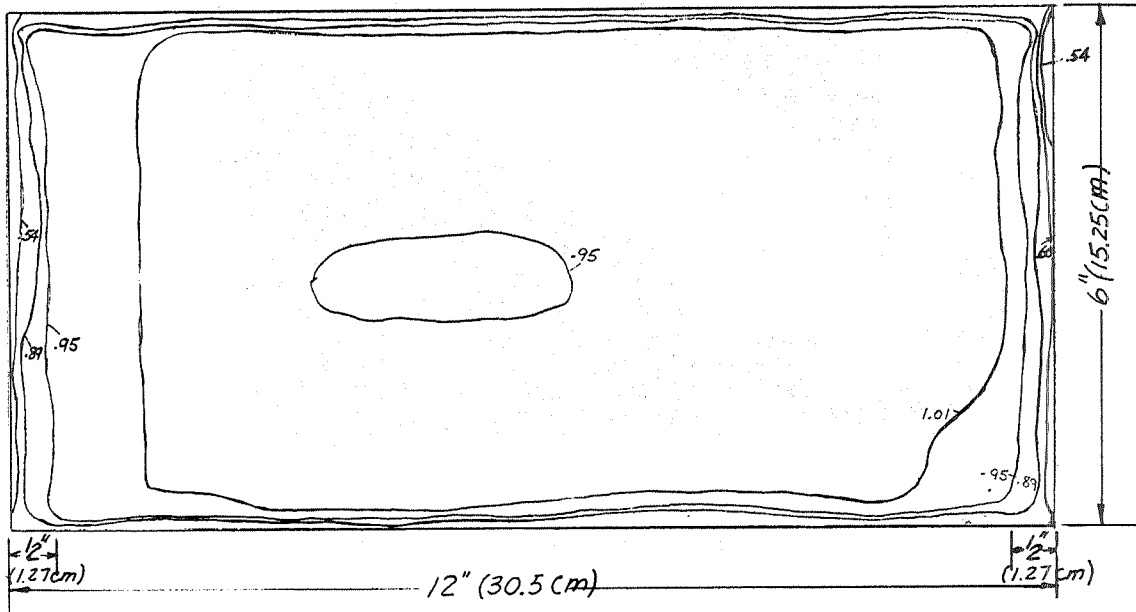


Figure 32. Exit plane velocity map for Griffith diffuser with area ratio = 2.

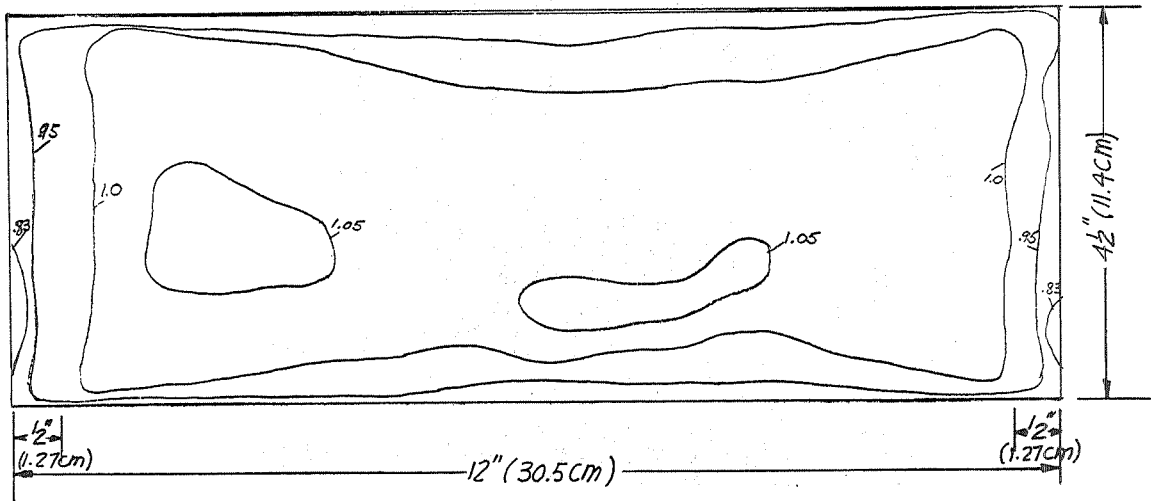


Figure 33. Exit plane velocity map for Griffith diffuser with area ratio = 3.

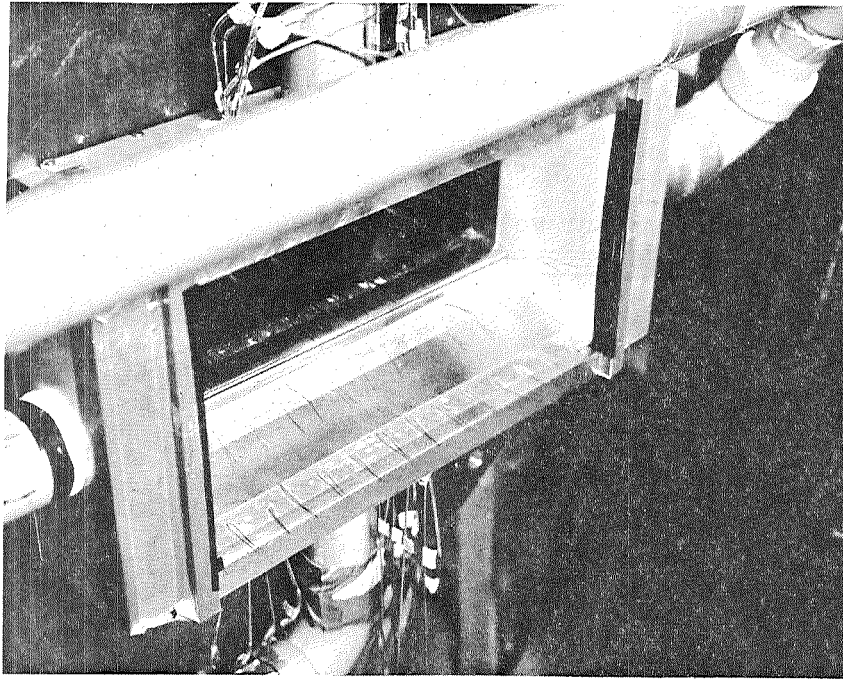


Figure 34. Tufts of string attached to Griffith diffuser wall indicate steadiness of flow when suction is applied.

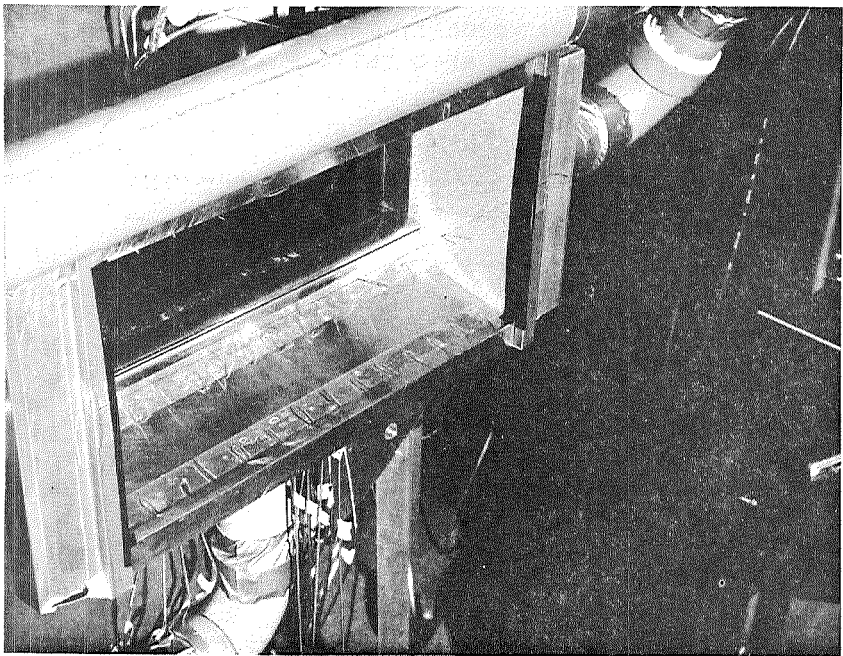


Figure 35. Motion of tufts indicate flow separation and reversal when no suction is applied.

Figures 32 and 33 show exit plane velocity maps for the diffuser with stable operation when operated with area ratios of 2 and 3 respectively. The contours of constant exit plane velocity exhibit a flat profile for the major portion of the exit flow. Figures 34 and 35 show photographs of the diffuser with and without slot suction. Tufts of string attached to the diffuser wall indicate the flow to be completely attached when adequate suction is applied. Flow separation and reversal are noted to occur when no suction is applied.

Figure 36 summarizes the effect of slot suction rate upon the diffuser effectiveness for area ratios of 2, 3 and 4 to 1. There is a minimum slot

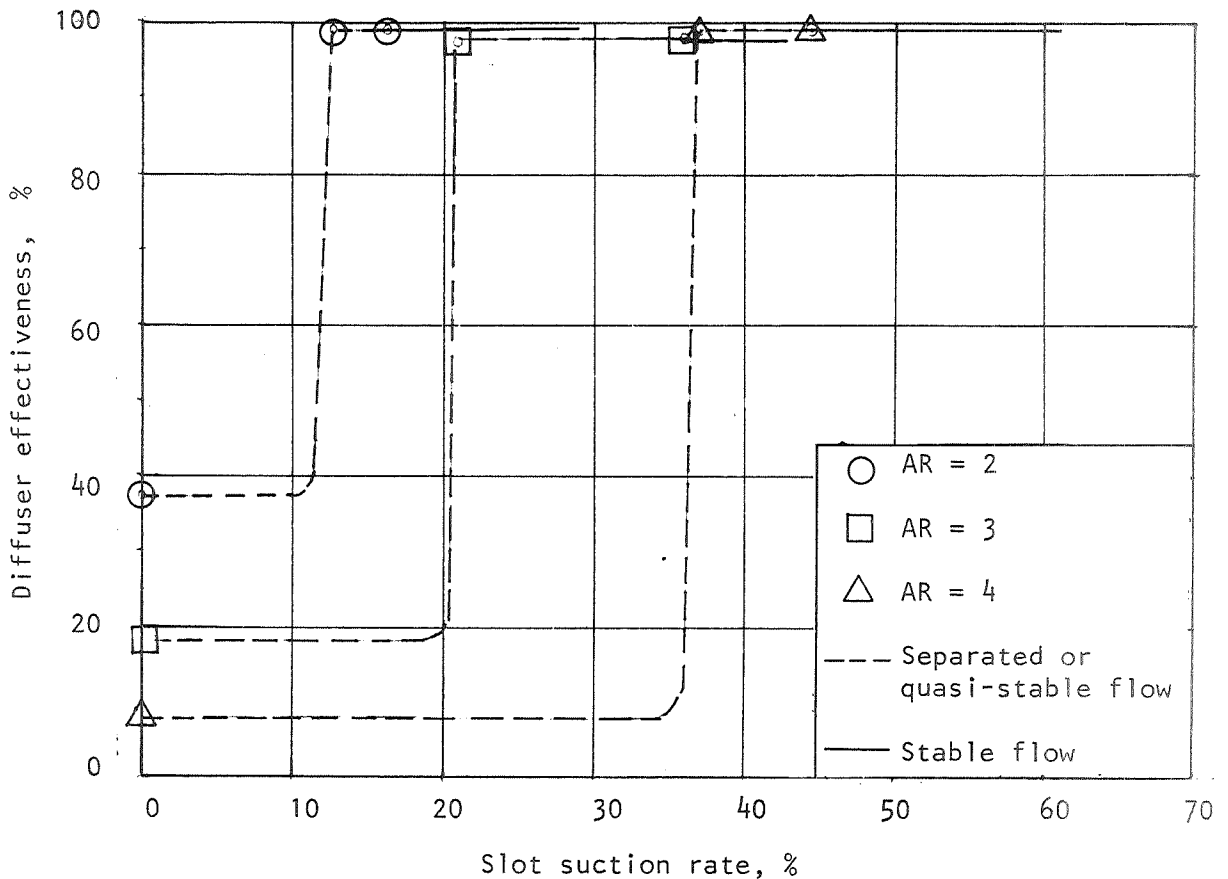


Figure 36. Effect of slot suction rate on Griffith diffuser performance.

suction rate required for unseparated flow for each area ratio. This minimum rate goes up significantly as the area ratio is increased. Below this minimum rate, the diffuser effectiveness is very low because separation occurs upstream of the suction slot. Increasing the suction rate has no appreciable effect until the minimum rate required for unseparated flow is surpassed. As previously discussed, only quasi-stable operation was possible with suction rates between the very minimum required for unseparated flow and the minimum required for completely stable operation.

It is believed that the following factors account for the high suction rates required by the Griffith diffuser. Each factor is related to the geometric design in the vicinity of the suction slot.

(1) The computer design program used had two weaknesses:

(a) It was somewhat inaccurate in the region of high velocity gradients. In this region, which included the suction slot, there were considerable differences between the wall velocities prescribed to the design program and the corresponding wall velocities computed by the analysis program. Reasonably good agreement was achieved between prescribed and predicted velocities for the regions upstream and downstream of the zone of deceleration.

(b) The program did not provide for the reduction in the diffuser flow rate downstream of the slot. If the branch flow out of the slot had been properly accounted for, the geometry in the vicinity of the slot would have been significantly affected, although the geometry far downstream from the slot would be only slightly affected.

(2) A sharp lip rather than a rounded lip was used downstream of the suction slot. This would be acceptable if the stagnation streamline separating slot flow from downstream diffuser flow could terminate precisely on the sharp edge. For stable flow, however, this is not feasible, and the stagnation streamline moves downstream of the lower lip. This in turn requires the flow between the stagnation streamline and the lower lip to make an "S" - shaped path in entering the slot. See Figure 37. A real fluid would likely separate unless additional suction is applied to enable the existence of a small "locked-in" eddy. This phenomenon is similar to the bubble around the leading edge of an airfoil when there is a flow reattachment. See Figure 38.

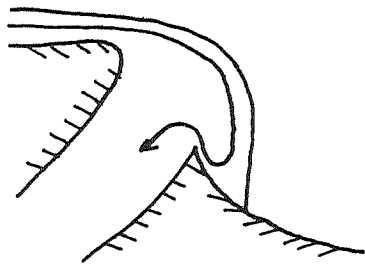


Figure 37. Flow pattern required at sharp lower lip.

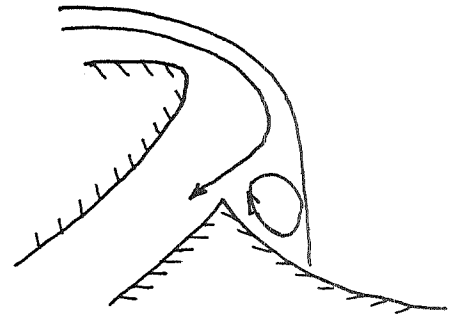


Figure 38. Locked-in eddy downstream of slot.

A volume flow balance was made on the Griffith diffuser with area ratios of 2 and 3. The inlet volume flow rates were determined from the inlet dynamic pressure measurements, the suction rates through each suction slot and each sidewall were measured individually by flow meters, and the

exit flow rates were determined from exit plane velocity measurements at 91 locations as mentioned in paragraph 4.4. The same velocity measurements were used to obtain the exit plane velocity maps shown as Figures 32 and 33. Table II shows the results of these tests.

TABLE II. GRIFFITH DIFFUSER FLOW RATE BALANCE

	AR = 2	AR = 3
Inlet flow rate	12.12 CFS (0.343 m ³ /sec)	6.95 CFS (0.196 m ³ /sec)
Suction flow rate	3.33 CFS (0.094 m ³ /sec)	2.33 CFS (0.066 m ³ /sec)
Exit flow rate	8.41 CFS (0.248 m ³ /sec)	4.09 CFS (0.116 m ³ /sec)

The difference between the inlet flow rate and the sum of the exit and suction flow rates was about 3.1% and 7.6% for AR = 2 and AR = 3 respectively.

6.3 CIRCULAR ARC DIFFUSER

Preliminary test runs on the circular arc diffusers with area ratios and various slot locations are summarized in the Appendix. These runs were used to determine the geometry resulting in highest diffuser effectiveness.

6.3.1 SINGLE-SLOT DIFFUSER

A summary of test runs with the selected geometry diffuser and of test runs with a double-slot diffuser is given in Table III.

Run numbers 7 through 18 involved tests on circular arc diffusers with one suction slot per curved wall and with an area ratio of 2.5. Inlet velocity was approximately 250 ft/sec (76.2 m/sec) and inlet Reynolds number was 230,000. The sidewall suction rate was about 3.5%, and the slot suction was varied from 0.0 to 10.0%.

Figures 39 and 40 show the results of run no. 7, which used 10% total slot suction through the two 3/16 inch (0.476 cm) slots. Figure 39 shows good correlation between the measured and predicted values of wall pressure coefficient and centerline velocity up to the vicinity of the junction of the circular arc wall and the exit plate. Considerable deviation between measured and predicted values occurs after this junction point. Figure 40 shows the horizontal and vertical velocity profiles taken at various planes downstream from the diffuser entrance. The horizontal velocity profiles indicate that the sidewall suction was adequate to maintain a two-dimensional flow pattern. The vertical velocity profiles indicate no flow reversal in the planes of velocity traverse, although the flow is skewed toward the bottom wall. The asymmetry of the flow was developed during the process of setting the test conditions. Once the flow was skewed toward one wall, a considerable excess of suction had to be applied to the opposite wall to shift the flow pattern. The diffuser effectiveness was 84.8% and the total pressure loss was 13.4% of the inlet dynamic pressure or 0.46% of the inlet total pressure.

Figures 41 and 42 show the results of run no. 8, which used the same diffuser as run no. 7, but with the slot suction rate reduced to 4.3%. The diffuser effectiveness was reduced from approximately 85% to 70%. Figure 41 indicates a larger deviation between measured and predicted centerline velocities for this run compared with the previous run. This was as expected, since flow separation and reversal were much more severe with the reduced slot suction used in this run. The vertical velocity profiles shown in Figure 42 verify the flow reversal and the resultant poor vertical velocity distribution. Some preference for the bottom wall is shown,

Run no. 7 3/16 in (0.476 cm) slot @ 15°
 $\eta = 84.8\%$ Slot suction = 10.0%
 $P_{loss} = 0.46\%$ $P_{t,i} = 14.627$ psia (756 mm Hg)

Area ratio = 2.5

$V_{inlet} = 254$ ft/sec (77.5 m/sec)

S.W. suction = 3.1%

Reynolds number = 230,000

$P_{s,i} = 14.128$ psia (730 mm Hg)

$P_{s,e} = P_a = 14.500$ psia (749 mm Hg)

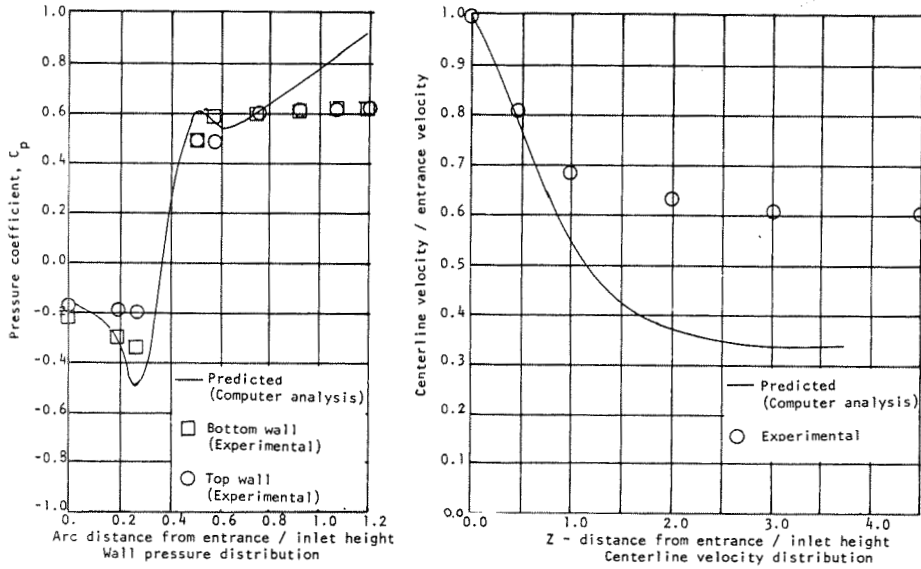


Figure 39. Wall pressure and centerline velocity distribution for circular arc diffuser with one slot per wall.

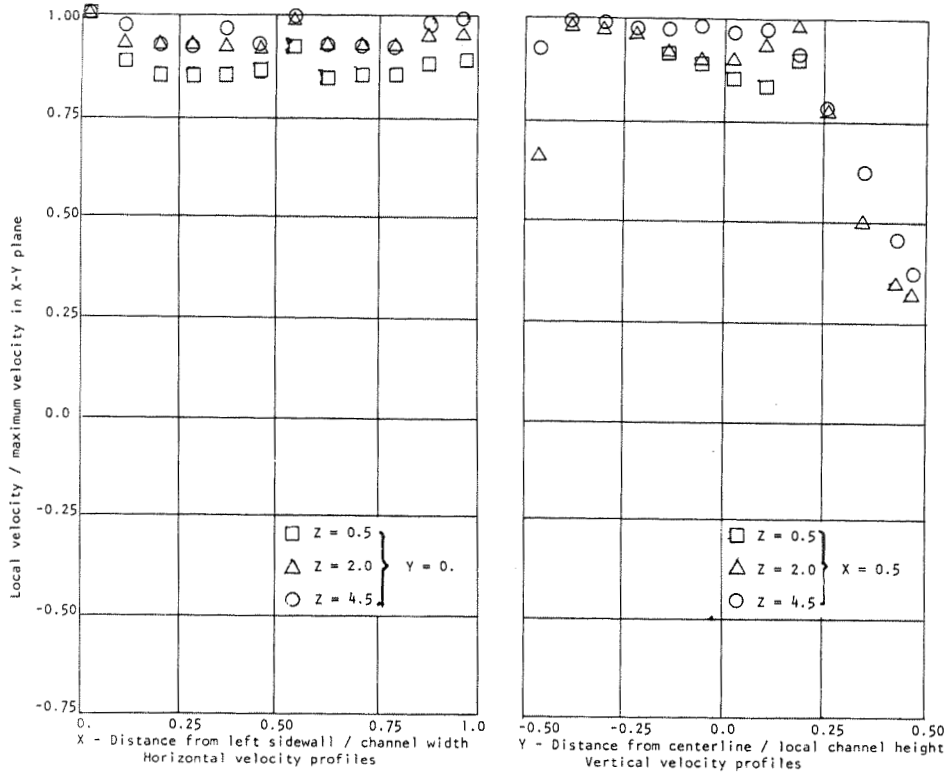


Figure 40. Velocity profiles for circular arc diffuser with one slot per wall.

Run no. 8 3/16 in (0.476 cm) slot @ 15°
 $n = 70.0\%$ Slot suction = 4.3%
 $P_{loss} = 0.89\%$ $P_{t,i} = 14.790$ psia (764 mm Hg)

Area ratio = 2.5
 S.W. suction = 3.3%
 $P_{s,i} = 14.284$ psia (738 mm Hg)

$V_{inlet} = 255$ ft/sec (77.7 m/sec)
 Reynolds number = 230,000
 $P_{s,e} = P_a = 14.590$ psia (754 mm Hg)

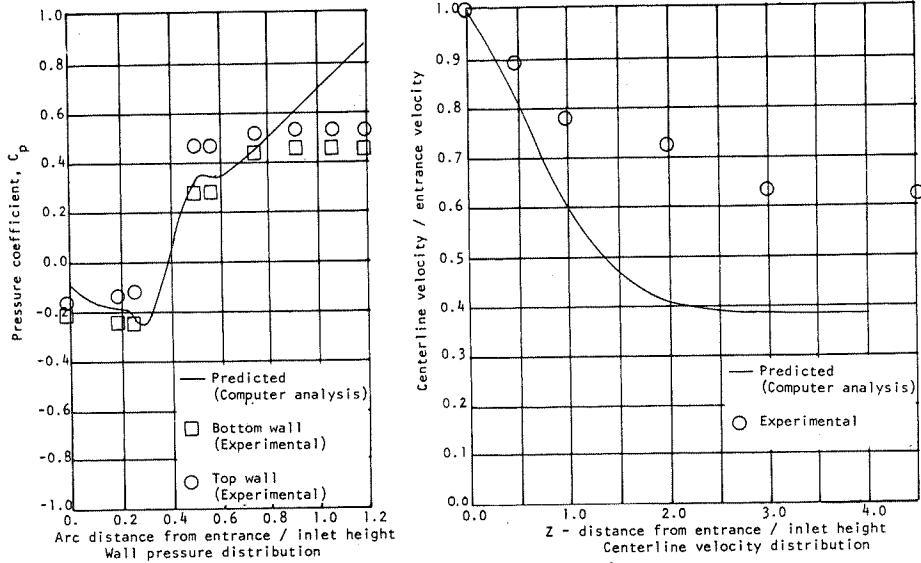


Figure 41. Wall pressure and centerline velocity distribution for circular arc diffuser with one slot per wall.

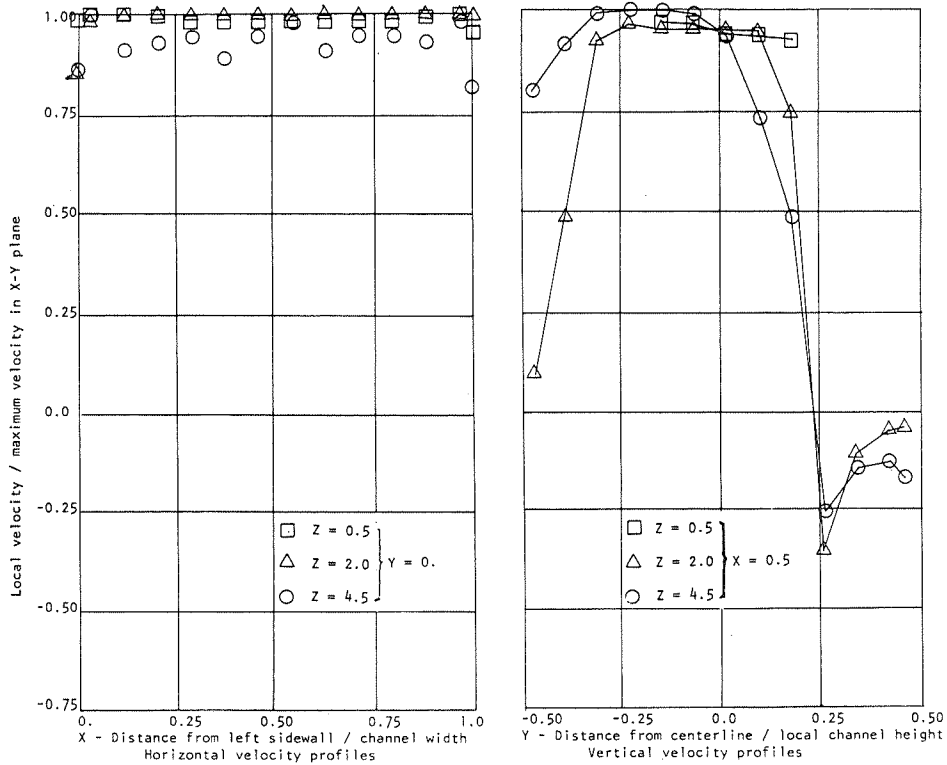


Figure 42. Velocity profiles for circular arc diffuser with one slot per wall.

particularly at the exit plane. The horizontal velocity profiles indicate again that the sidewall suction enabled the existence of a two-dimensional flow pattern.

Figures 43 and 44 show the results of run no. 9, which utilized no slot suction. The diffuser effectiveness dropped to 26%. The early deviation between measured and predicted centerline velocities indicates early flow separation -- probably in the vicinity of the suction slot. The vertical velocity profiles indicate a very poor vertical velocity distribution, with severe flow distortion and reversal. The horizontal velocity profiles show that a reasonably well-established two-dimensional flow pattern existed in spite of the poor vertical distribution.

Run numbers 10, 11, and 12 were similar to run numbers 7, 8, and 9, except that a 1/16 inch (0.159 cm) continuous slot was used for suction instead of a 3/16 inch (0.476 cm) continuous slot. The behavior of the diffuser was very nearly the same for the two slot sizes when equal suction rates were applied.

Run numbers 13, 14, and 15 utilized 3/16 inch (0.476 cm) diameter holes spaced 0.281 inch (0.715 cm) apart for slot suction. Figures 45 and 46 show the results when 9.1% slot suction and 3.4% sidewall suction was applied. The diffuser effectiveness was 59.5%, compared with 84.8% when using a continuous slot and applying equal suction rates. Sufficient slot suction was applied to result in a reasonably distributed (nearly full channel) flow. A considerably higher adverse pressure gradient existed along the curved wall with distributed flow than with little or no slot suction. The lack of slot suction near the junction of the sidewall and the row of holes caused separation to occur near the sidewall. The

Run no. 9 3/16 in (0.476 cm) slot @ 15° Area ratio = 2.5 $V_{inlet} = 252 \text{ ft/sec (76.8 m/sec)}$
 $n = 26.0\%$ Slot suction = 0.0% S.W. suction = 3.2% Reynolds number = 230,000
 $P_{loss} = 2.12\%$ $P_{t,i} = 15.084 \text{ psia (779 mm Hg)}$ $P_{s,i} = 14.578 \text{ psia (753 mm Hg)}$ $P_{s,e} = P_a = 14.690 \text{ psia (759 mm Hg)}$

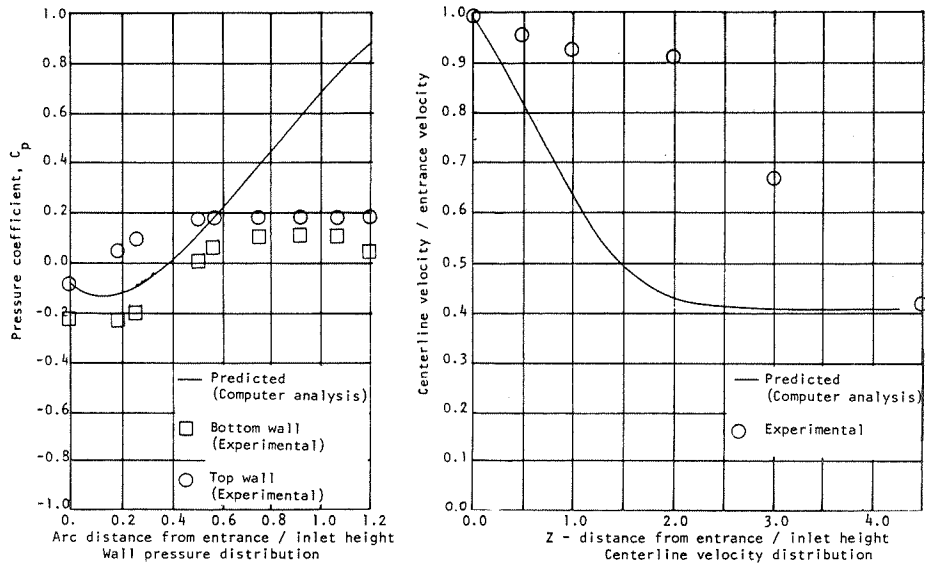


Figure 43. Wall pressure and centerline velocity distribution for circular arc diffuser with one slot per wall.

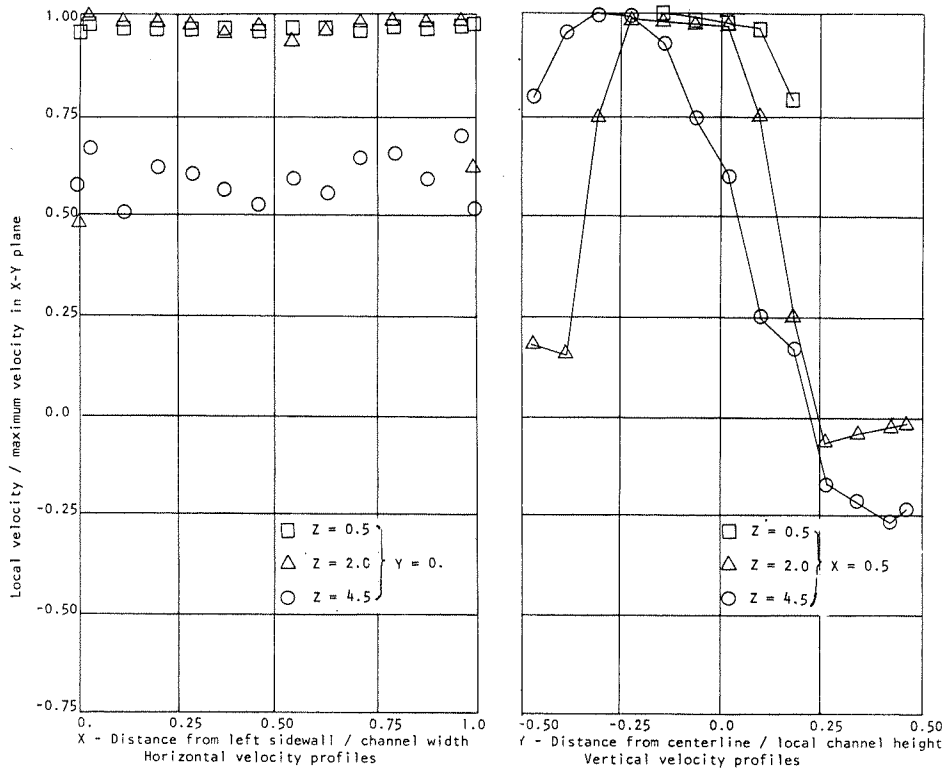


Figure 44. Velocity profiles for circular arc diffuser with one slot per wall.

Run no. 13 3/16 in (0.476 cm) holes @ 15° Area ratio = 2.5 $V_{inlet} = 253 \text{ ft/sec (77.2 m/sec)}$
 $n = 59.5\%$ Slot suction = 9.1% S.W. suction = 3.4% Reynolds number = 230,000
 $P_{loss} = 1.20\%$ $P_{t,i} = 14.839 \text{ psia (767 mm Hg)}$ $P_{s,i} = 14.338 \text{ psia (741 mm Hg)}$ $P_{s,e} = P_a = 14.600 \text{ psia (755 mm Hg)}$

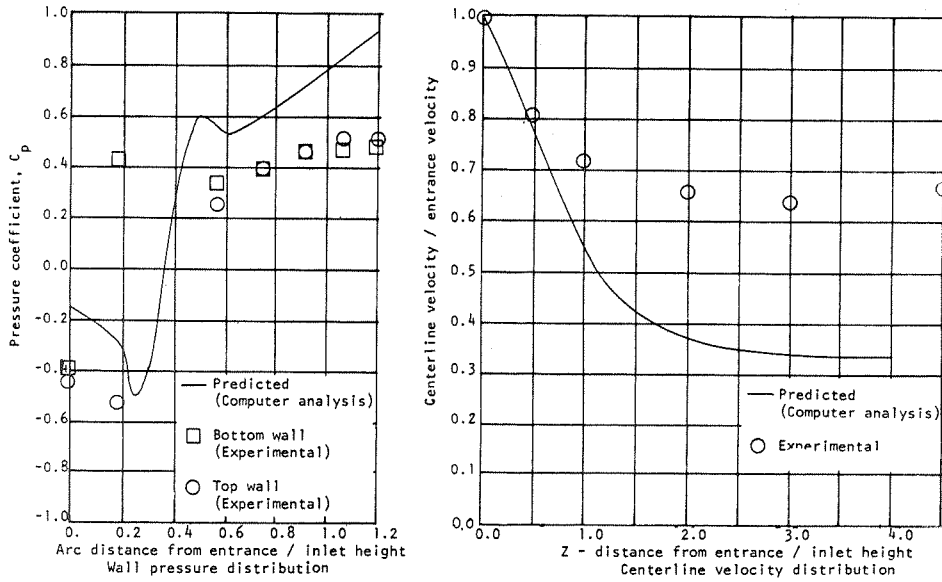


Figure 45. Wall pressure and centerline velocity distribution for circular arc diffuser with 3/16" suction holes.

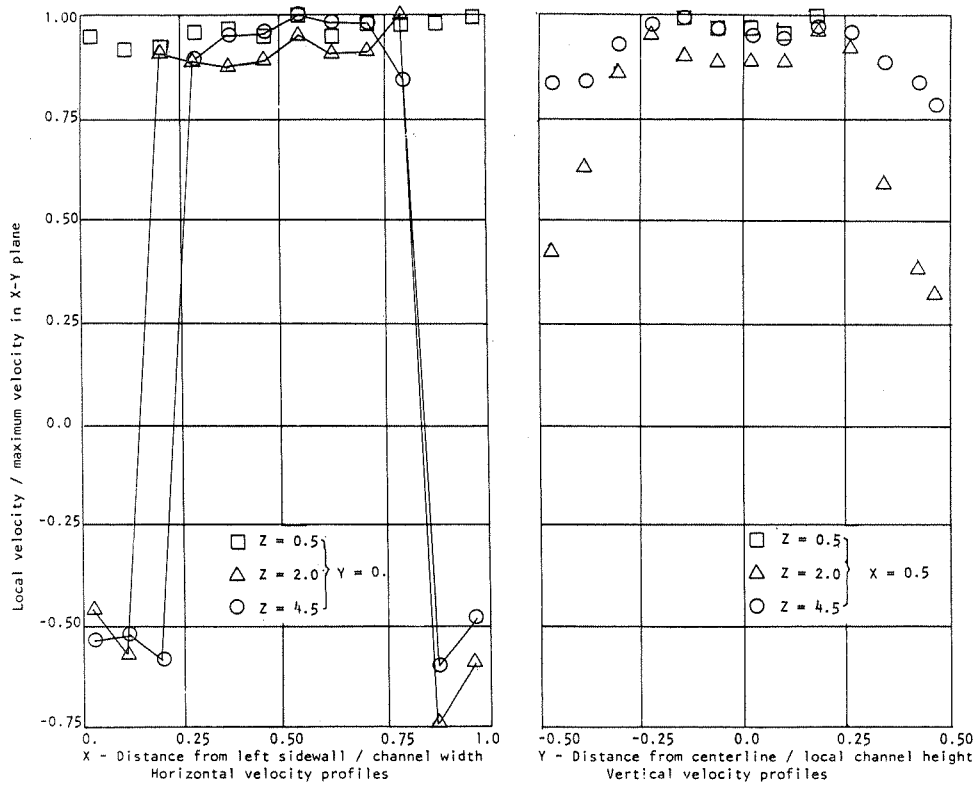


Figure 46. Velocity profiles for circular arc diffuser with 3/16" suction holes.

horizontal velocity profiles show this separation and flow reversal. A two-dimensional flow pattern was obviously not achieved. If the geometry had been arranged so as to have a half-hole at each end of the row of suction holes, the separation near the sidewall probably would not have occurred.

Runs 16, 17, and 18 were similar to runs 13, 14, and 15 except that 1/16 inch (0.157 cm) holes spaced .0937 inch (0.238 cm) apart were used for slot suction. Again, the diffuser effectiveness was considerably lower than when a continuous slot was used with equal suction rates.

A volume flow rate balance was made for test no. 7, with the results shown in Figure 47. Good agreement is indicated for the various transverse planes of measurement. A maximum deviation of approximately 3% occurred at the plane $Z = 2.0$. Several additional volume flow rate balances were made, but the results were not as good as test no. 7. Generally, the results became poorer as flow separation and reversal became more severe.

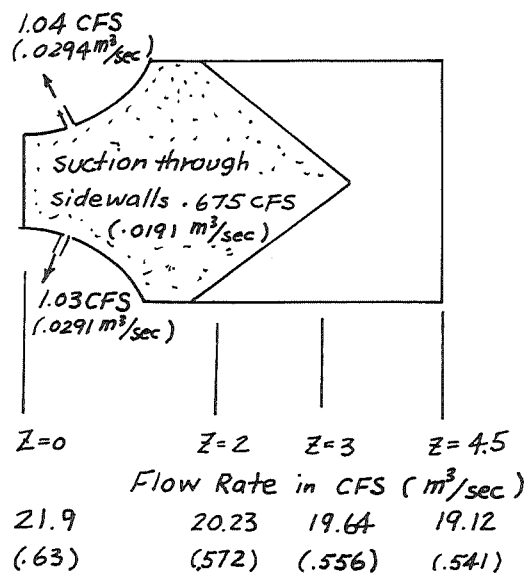


Figure 47. Measured flow rates at various transverse planes for run no. 7.

6.3.2 DOUBLE-SLOT DIFFUSER

Test numbers 19 through 23 were made on a circular arc diffuser having two slots per curved wall. The first slot was 3/16 inch (0.476 cm) wide and located 15° from the diffuser entrance; the second slot was 1/16 inch (0.159 cm) wide and located 50° from the diffuser entrance. All tests were made with an inlet velocity of 250 ft/sec (76.2 m/sec) and an area ratio of 4 to 1. With this area ratio, each curved wall was a complete quarter-cylinder.

Figures 48 and 49 show the results for test no. 19, which used a total slot suction rate of 9.54%. The vertical velocity profiles and the center-line velocity distribution indicate that the flow distribution is skewed toward the bottom wall. The preference of the flow for top or bottom wall was discussed in paragraph 6.3.1. The diffuser effectiveness was 46.6%, which was considerably less than the 72.5% effectiveness obtained in preliminary test no. 3 (see Appendix). This preliminary run was made with the same test conditions as run no. 19, but only one suction slot was used in the preliminary test.

Tests 20 through 23 used less slot suction than test 19, resulting in even lower values of diffuser effectiveness. The double-slot test runs were thus not successful in improving diffuser performance over that obtained with a single slot per wall. The inflexibility in relative slot location and independent slot suction rate control prevented final conclusions from being reached on the feasibility of two slots per wall. It is apparent that the downstream slot was not effective, and might have been effective only if located farther upstream.

Run no. 19 3/16 in (0.476 cm) slot @ 15° Area ratio = 4.0 $V_{inlet} = 252 \text{ ft/sec (76.8 m/sec)}$
 1/16 in (0.159 cm) slot @ 50°
 $n = 46.6\%$ Slot suction = 9.54% S.W. suction = 3.5% Reynolds number = 230,000
 $P_{loss} = 1.71\%$ $P_{t,i} = 14.877 \text{ psia (770 mm Hg)}$ $P_{s,i} = 14.378 \text{ psia (744 mm Hg)}$ $P_{s,e} = P_a = 14.600 \text{ psia (755 mm Hg)}$

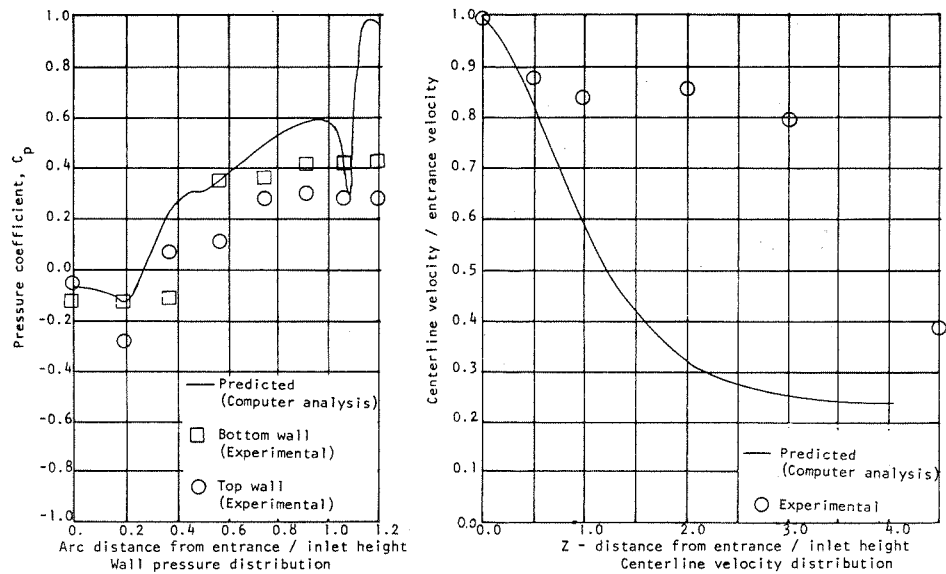


Figure 48. Wall pressure and centerline velocity distribution for circular arc diffuser with two slots per wall.

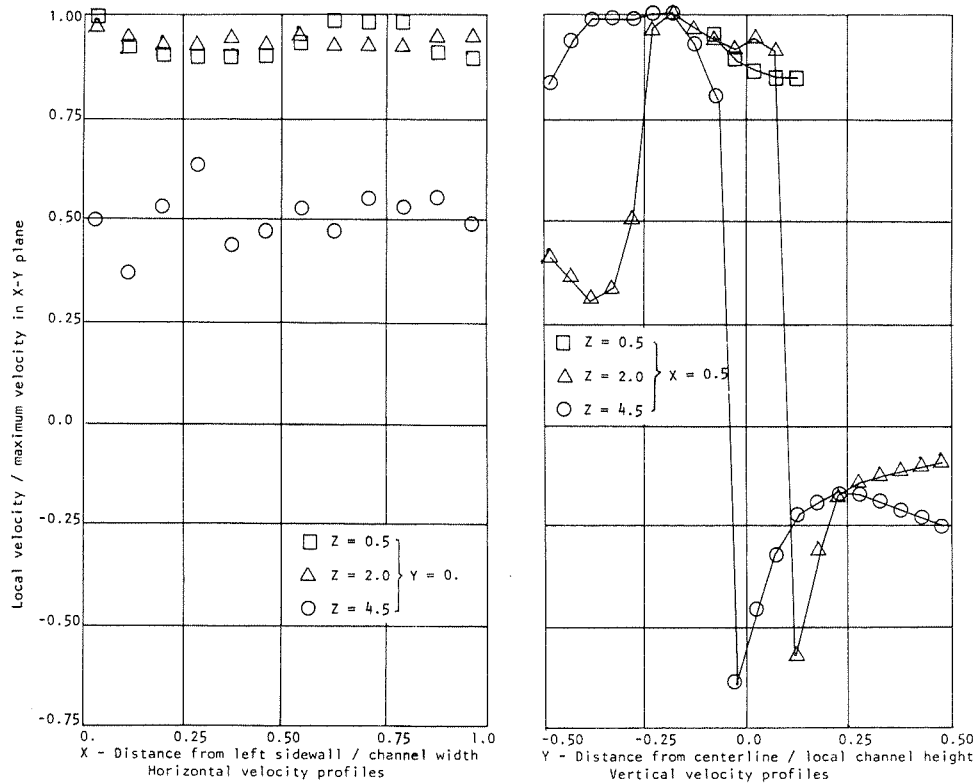


Figure 49. Velocity profiles for circular arc diffuser with two slots per wall.

6.3.3 CIRCULAR ARC DIFFUSER SUMMARY

Table III summarizes the results of tests made on the circular arc diffuser.

TABLE III. CIRCULAR ARC DIFFUSER TEST RESULTS*

Test No.	Slot Geometry	Area Ratio	Inlet Velocity		% Suction	
			Ft/sec	M/sec	Slots	Sidewalls
7	3/16" (0.476 cm) continuous @ 15°	2.5	254	77.5	10.0	3.1
8	3/16" (0.476 cm) continuous @ 15°	2.5	255	77.7	4.3	3.3
9	3/16" (0.476 cm) continuous @ 15°	2.5	252	76.8	0.0	3.2
10	1/16" (0.159 cm) continuous @ 15°	2.5	254	77.5	8.5	3.6
11	1/16" (0.159 cm) continuous @ 15°	2.5	254	77.5	5.3	3.3
12	1/16" (0.159 cm) continuous @ 15°	2.5	252	76.8	0.0	3.3
13	3/16" (0.476 cm) holes @ 15°	2.5	253	77.2	9.1	3.4
14	3/16" (0.476 cm) holes @ 15°	2.5	253	77.2	5.2	3.8
15	3/16" (0.476 cm) holes @ 15°	2.5	252	76.8	0.0	4.0
16	1/16" (0.159 cm) holes @ 15°	2.5	252	76.8	8.5	2.2
17	1/16" (0.159 cm) holes @ 15°	2.5	252	76.8	5.1	3.8
18	1/16" (0.159 cm) holes @ 15°	2.5	253	77.2	0.0	3.8

* All test runs were made with an inlet Reynolds number of 230,000.

TABLE III
(Cont'd)

Test No.	Slot Geometry	Area Ratio	Inlet Velocity		% Suction	
			Ft/sec	M/sec	Slots	Sidewalls
19	3/16" (0.476 cm) continuous @ 15° 1/16" (0.159 cm) continuous @ 50°	4.0	252	76.8	9.5	3.5
20	"	4.0	253	77.2	6.9	3.8
21	"	4.0	253	77.2	5.2	3.8
22	"	4.0	253	77.2	3.3	3.8
23	"	4.0	253	77.2	0.0	3.9

Test No.	Total Inlet Pressure		$(\Delta P)_{\text{static}}$ $P_{s,e} - P_{s,i}$		Total Pressure Loss % of Inlet		Effectiveness η %
	Psia	mm Hg	Psi	mm Hg	Dynamic	Total	
7	14.627	755	0.372	19.2	13.4	0.46	84.8
8	14.790	764	0.306	15.8	25.9	0.89	70.0
9	15.084	779	0.112	5.8	63.0	2.12	26.0
10	14.735	762	0.368	19.0	14.6	0.50	83.3
11	14.713	762	0.317	16.4	23.1	0.79	73.3
12	14.877	770	0.142	7.4	56.5	1.90	33.5
13	14.839	767	0.262	13.5	35.6	1.20	59.5
14	14.857	769	0.242	12.5	38.2	1.29	55.9
15	14.997	776	0.106	5.5	64.1	2.15	24.8
16	14.856	769	0.243	12.5	38.5	1.29	55.9
17	14.766	763	0.232	12.0	40.1	1.36	53.6
18	14.961	774	0.130	6.7	59.3	2.00	30.4
19	14.877	770	0.222	11.5	50.9	1.71	46.6
20	14.917	771	0.184	9.5	58.3	2.00	38.6
21	14.942	773	0.159	8.1	63.1	2.12	33.4
22	14.969	774	0.132	6.8	68.3	2.29	27.8
23	15.016	777	0.085	4.4	77.2	2.58	18.0

Figure 50 summarizes the effect of slot suction rate upon diffuser effectiveness for the various circular arc geometries tested. For an area ratio of 2.5 and with continuous suction slots, the diffuser effectiveness increases from approximately 30% to 85% as the percentage suction increases from 0% to 10%. As shown in the Appendix, preliminary test runs indicated a maximum effectiveness of 87.4% for this geometry. Using holes instead of a continuous slot but with the same area ratio, the diffuser effectiveness

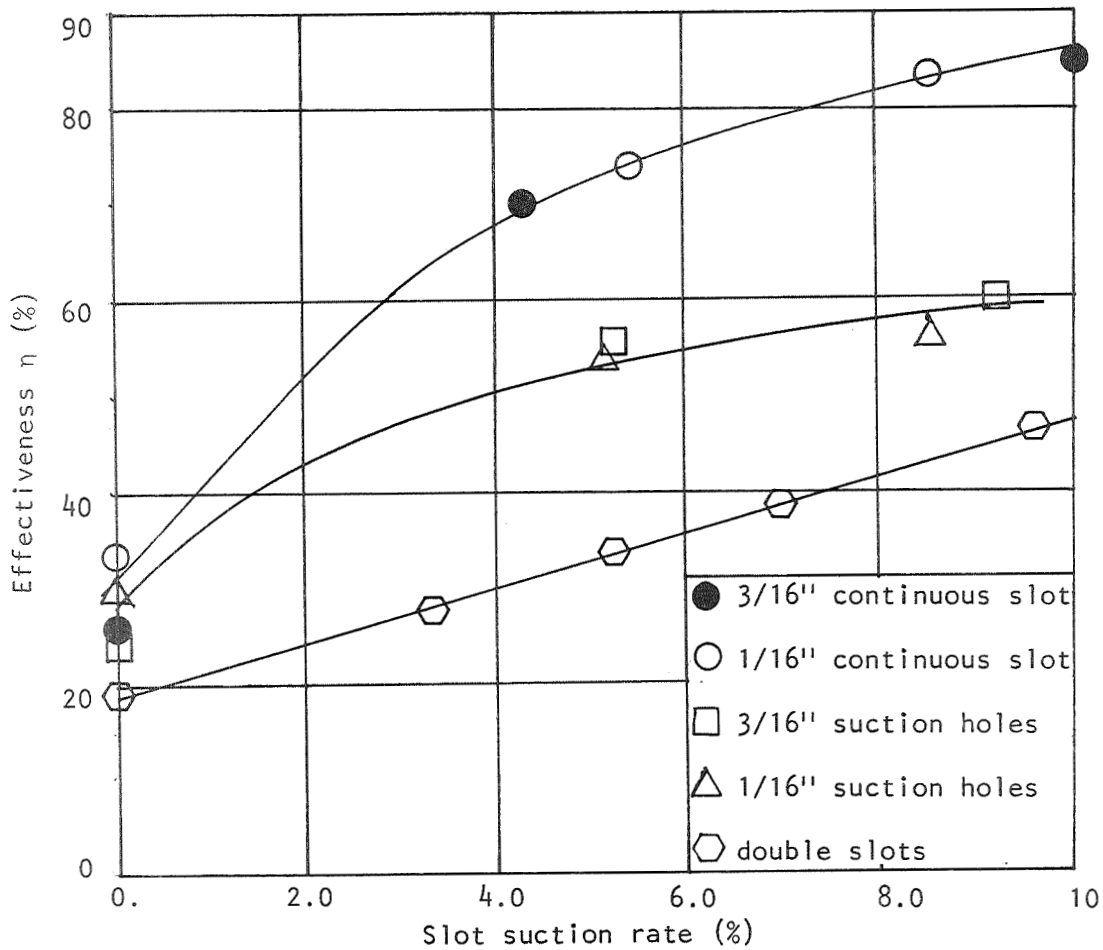


Figure 50. Effect of slot suction rate on circular arc diffuser performance.

increases from approximately 30% to 60% as the percentage suction increases from 0% to 10%. With the double-slot configuration and an area ratio of 4.0, the effectiveness increased from approximately 18% to 47% with the same range of suction rates. For this configuration, however, neither the slot positions nor the relative slot suction rates were necessarily optimized.

In order to determine the transition Reynolds number, a set of tests were made on the circular arc diffuser having a 3/16 inch (0.476 cm) continuous slot. The area ratio was 2.5, and the suction percentages were maintained constant at approximately 10% and 3% through the slots and side-walls respectively. Inlet velocities were varied from 30 ft/sec (9.1 m/sec) to 250 ft/sec (76.2 m/sec), corresponding to a variation in inlet Reynolds number from 30,000 to 230,000. Figure 51 shows the results of these tests.

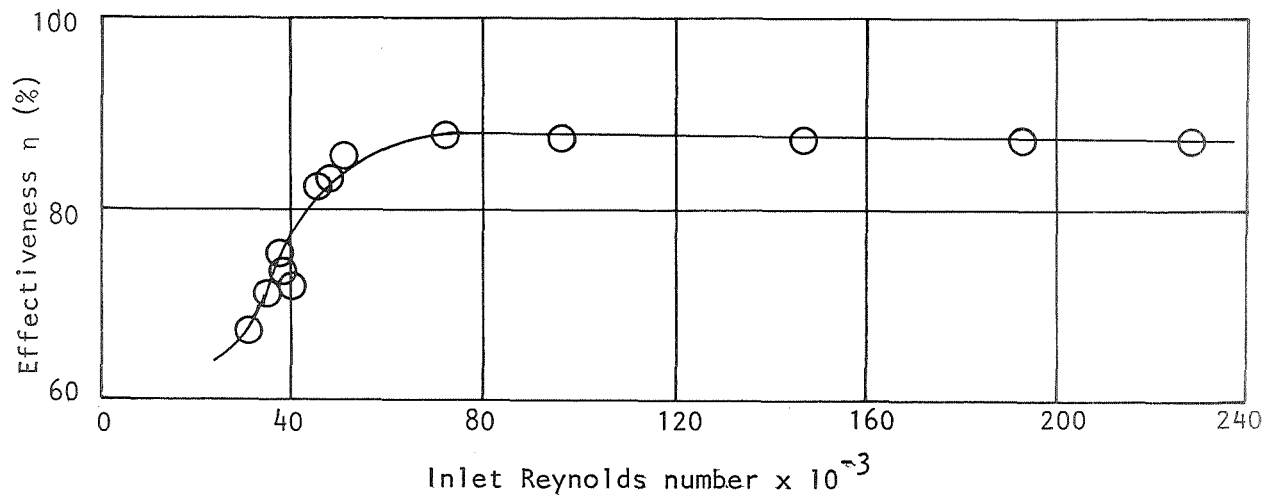


Figure 51. Effect of Reynolds number on circular arc diffuser performance.

There is apparently a transition region in the range of Reynolds numbers from 30,000 to 50,000, after which the diffuser effectiveness is essentially constant. For practical consideration, the diffuser effectiveness is virtually independent of Reynolds number since the transition range is very low.

SECTION VII

CONCLUSIONS

The application of slot suction in short two-dimensional curved wall diffusers to improve performance was investigated. The performance of two diffuser designs was evaluated experimentally.

7.1 GRIFFITH DIFFUSER

Experimental results indicate that a two-dimensional diffuser utilizing the concept of a concentrated deceleration zone incorporated with slot suction is feasible if sufficient suction can be applied to prevent flow separation. A nearly uniform exit velocity distribution and a diffuser effectiveness of approximately 98% were achieved when operating with exit area to inlet area ratios of 2, 3 and 4 to 1 and suction rates up to 45% of the inlet flow. The correlation between measured values of velocity and wall pressure and values predicted by potential flow analyses was very good when sufficient suction was applied to prevent flow separation.

The slot suction rate required for stable unseparated flow was 16% at an area ratio of 2. Quasi-stable unseparated flow was achieved with a slot suction rate as low as 12%. If a flow disturbance caused separation, the suction rate had to be increased again to 16% to restore the unseparated

flow. For operation at area ratios of 3 and 4, the corresponding suction rates were 36% and 45% for stable operation. The authors believe that the primary reason for the significantly higher suction rate percentages at the higher area ratios might be the smaller volume flow through the smaller inlet area of the test diffuser which was used for higher area ratios. The total volume removed by suction was only slightly higher at higher area ratios than at lower area ratios.

In all cases, the diffuser performance decreased abruptly when the suction rate was inadequate to maintain unseparated flow. The reason for the suction rate being higher than the estimated minimum is assumed to lie partly in the difficulty of designing an optimum slot geometry. Combining potential flow and boundary layer analyses including suction into one design program should lead to a diffuser requiring a smaller suction rate for unseparated flow.

7.2 CIRCULAR ARC DIFFUSER

The effectiveness of the circular arc diffuser was increased from approximately 30% to 85% by increasing the slot suction rate from 0% to 10% while operating with an exit area to inlet area ratio of 2.5 to 1. This ratio was near the upper limit if the flow pattern at the diffuser exit was restricted to being stable and distributed, and the suction rate was restricted to 10%.

The optimum location of the suction slot was 15° from the diffuser entrance, which was near the location of flow separation when no suction was applied.

No large difference in diffuser performance was observed between the use of suction slot widths of 3/16 inch and 1/16 inch. Continuous slots

were more effective than closely spaced holes when using the same percentage suction rate. When holes were used the influence of the suction was not uniformly distributed. Thus there were regions with inadequate suction, particularly at the junctions of the curved walls and the sidewalls. In all tests which used suction holes, separation occurred in those regions.

A reasonably good correlation between potential flow analysis prediction and experimental results of velocity and pressure distribution existed upstream of flow separation. Downstream of separation, predicted and experimental results diverged as expected.

The double-slot test runs were not successful in verifying the design concept of using two slots per curved wall for higher area ratios such as 4. This was primarily because the test set-up did not provide for moving the location of the downstream slot relative to the upstream slot nor did it provide for independent control of the suction rate through the two slots. The upstream slot should have received a higher percentage of the suction flow. The downstream slot, which was located at 50° , might have been effective only if located farther upstream. Considerable flow separation and reversal occurred resulting in a diffuser effectiveness of only 47% at 10% suction.

SECTION VIII

REFERENCES

1. Ringleb, F.O., "Two-Dimensional Flow with Standing Vortices in Ducts and Diffuser," Journal of Basic Engineering, Trans. of ASME, Pages 921-928, Series D, Vol. 82, 1960.
2. Kline, S.J., Abbott, D.E. and Fox, R.W., "Optimum Design of Straight Walled Diffusers," Trans. of ASME, Series D, Journal of Basic Engineering, Vol. 81, No. 3, September, 1959.
3. McDonald, A.T. and Fox, W.F., "Incompressible Flow in Conical Diffusers," Technical Report No. 1, Purdue Research Foundation, Lafayette, Indiana, September, 1964.
4. Cochran, D.L. and Kline, S.J., "Use of Short Flat Vanes for Producing Efficient Wide-Angle Two-Dimensional Subsonic Diffusers," NACA TN 4309, 1958.
5. Yang, T., "Splitter Effect in Conical Diffusers, Part II Optimum Design Procedure," Clemson University, Engineering Bulletin 106, 1966.
6. Valentine, E.F. and Carroll, R.B., "Effects of Some Primary Variables of Rectangular Vortex Generators on Static Pressure Rise through a Short Diffuser," NACA RM L52B 13, 1954.
7. Manoni, L.R., "Wide Angle Diffuser Employing Boundary Layer Control," Report R-95460-12, United Aircraft Corp. Research Department, March, 1952.
8. G.V. Lachmann, Boundary Layer and Flow Control, Pergamon Press, Vol. 1, Page 119.
9. Glauert, M.B., "The Design of Suction Airfoils with a Very Large C_L Range," R M No. 2111, Aeronautical Research Council, November, 1945.
10. Goldstein, S., "Low Drag and Suction Airfoils," Journal of Aeronautical Sciences, Vol. 15, No. 4, April, 1948.
11. Stanitz, J.D., "Design of Two-Dimensional Channels with Prescribed Velocity Distributions along the Channel Walls," NACA Report 1115, 1953.
12. Hess, J.L. and Smith, A.M.O., "Calculation of Potential Flow about Arbitrary Bodies," Progress in Aeronautical Sciences, Vol. 8, D. Kuchemann, ed., Pergamon Press, 1967, Pages 1-138.

APPENDIX

PRELIMINARY PERFORMANCE TESTS ON CIRCULAR ARC DIFFUSER

Run No.	Slot Size	Slot Location	% Suction Slot	% Suction Sidewall	Area Ratio	Effectiveness η , %	Flow Pattern
P1	3/16"	15°	0.0	0.0	4.00	23.2	Exited at center
P2	3/16"	15°	9.2	0.0	4.00	56.0	Exited at center
P3	3/16"	15°	9.7	3.2	4.00	72.5	Stable, attached to bottom
P4	3/16"	15°	0.0	0.0	3.00		Exited at center
P5	3/16"	15°	9.4	0.0	3.00	58.1	Exited at center
P6	3/16"	15°	9.6	3.1	3.00	80.2	Stable, attached to bottom
P7	3/16"	15°	9.7	0.0	2.75	60.1	Exited at center
P8	3/16"	15°	9.7	3.0	2.75	84.9	Stable and distributed
P9	3/16"	15°	9.9	0.0	2.50	62.0	Exited at center
P10	3/16"	15°	8.4	2.8	2.50*	85.5	Distributed and stable
P11	3/16"	15°	9.7	3.2	2.50*	87.4	Distributed and stable
P12	3/16"	20°	9.5	0.0	4.00	56.0	Exited at center
P13	3/16"	20°	10.1	3.1	4.00	68.8	Unstable
P14	3/16"	20°	9.7	0.0	3.00	59.2	Exited at center
P15	3/16"	20°	10.0	3.2	3.00	79.1	Stable, attached to bottom

APPENDIX
(Cont'd)

Run No.	Slot Size	Slot Location	% Suction		Area Ratio	Effectiveness η , %	Flow Pattern
			Slot	Sidewall			
P16	3/16"	20°	9.7	0.0	2.75	59.5	Exited at center
P17	3/16"	20°	9.3	3.0	2.75	81.5	Stable, attached to bottom
P18	3/16"	20°	9.7	3.2	2.75	76.0	Unstable
P19	3/16"	20°	9.7	0.0	2.50	61.4	Exited at center
P20	3/16"	20°	7.8	3.0	2.50	82.3	Stable, attached to bottom
P21	3/16"	20°	8.3	3.1	2.50	78.5	Unstable
P22	3/16"	25.7°	10.0	0.0	4.0	41.4	Unstable
P23	3/16"	25.7°	10.1	3.3	4.0	36.7	Attached to top wall
P24	3/16"	25.7°	10.2	0.0	3.0	51.1	Exited at center
P25	3/16"	25.7°	10.3	3.2	3.0	46.4	Attached to top wall
P26	3/16"	25.7°	10.2	0.0	2.75	52.2	Exited at center
P27	3/16"	25.7°	10.2	3.1	2.75	50.0	Attached to top
P28	3/16"	25.7°	10.4	0.0	2.5	55.7	Exited at center
P29	3/16"	25.7°	10.2	3.1	2.5	56.8	Separated from top
P30	1/16"	15°	7.6	3.4	4.0	67.1	Separated from top
P31	1/16"	15°	7.7	3.3	3.0	72.5	Separated from top

APPENDIX
(Cont'd)

Run No.	Slot Size	Slot Location	% Suction Slot	Suction Sidewall	Area Ratio	Effectiveness η , %	Flow Pattern
P32	1/16"	15°	8.0	3.3	2.75	78.4	Separated from top
P33	1/16"	15°	8.0	3.3	2.50*	84.1	Distributed
P34	1/16"	15°	8.5	3.4	2.50*	85.1	Distributed

* Best performance geometry

FINAL REPORT DISTRIBUTION LIST FOR NASA CR-120783; Contract NAS 3-13486

1. NASA-Lewis Research Center
 21000 Brookpark Road
 Cleveland, Ohio 44135
 Attention: Report Control Office MS 5-5 1
 Technology Utilization 3-19 1
 Library 60-3 2
 Fluid Systems Components Division 5-3 1
 W.L. Stewart 77-2 1
 J. Howard Childs 60-4 1
 L. Schopen 77-3 1
 J.B. Esgar 60-4 1
 H.H. Ellerbrock 60-4 1
 W.T. Olson 3-16 1
 R.A. Rudey 60-6 1
 J.F. Dugan, Jr. 501-2 1
 Seymour Lieblein 100-1 1
 R.E. Jones 60-6 1
 Jack Grobman 60-6 1
 Maj. R.C. Chaplin 501-3 1
 Lt. Col. C.S. Weden 500-317 1
 C.J. Marek 60-2 1
 James D. Holdeman 60-6 1
 James A. Albers 100-1 1
 David N. Anderson 60-2 1
 A.J. Juhasz 60-6 15

2. S. C. Fiorello
 Aeronautical Engine Laboratory
 Naval Air Engineering Center
 Philadelphia, Pennsylvania 19112 1

3. Aerospace Research Laboratory
 Wright-Patterson AFB, Ohio 45433
 Attention: Dr. R. G. Dunn 1

4. NASA Scientific and Technical Information Facility
 P. O. Box 33
 College Park, Maryland 20740
 Attention: NASA Representative
 RQT-2448 10

5. The Johns Hopkins University
 Applied Physics Laboratory
 8621 Georgia Avenue
 Silver Spring, Maryland 20910
 Attention: W. B. Shippen 1
 Dr. Gordon Dugger 1

6. NASA Headquarters
600 Independence Avenue, S. W.
Washington, D. C. 20546
Attention: N. F. Rekos (RAP) 1
 W. H. Roudebush (RAA) 1
7. Department of the Army
U. S. Army Aviation Material Laboratory
Propulsion Division (SAUFE-PP)
Fort Eustis, Virginia 23604
Attention: J. White 1
 E. T. Johnson 1
8. United Aircraft of Canada, Ltd
P. O. Box
Lonquenil, Quebec, Canada
Attention: Miss Mary Cullen 1
9. Air Force Office of Scientific Research
1400 Wilson Boulevard
Arlington, Virginia 22209
Attention: SREP 1
10. Defense Documentation Center (DDC)
Cameron Station
5010 Duke Street
Alexandria, Virginia 22314 1
11. Department of the Navy
Bureau of Naval Weapons
Washington, D. C. 20025
Attention: Robert Brown, RAPP14 1
12. Department of the Navy
Bureau of Ships
Washington, D. C. 20360
Attention: G. L. Graves 1
13. NASA-Langley Research Center
Langley Station
Technical Library
Hampton, Virginia 23365
Attention: Mark R. Nichols 1
 John V. Becker 1
 Richard J. Margajon MS 404 1

14. United States Air Force
 Aero Propulsion Laboratory
 Area B, Bldg. 18D
 Wright-Patterson A.F.B.
 Dayton, Ohio 45433
 Attention: Robert E. Henderson 1
15. United Aircraft Corporation
 Pratt & Whitney Aircraft Division
 400 Main Street
 East Hartford, Connecticut 06108
 Attention: G. Andreini 1
 Library 1
 R. Marshall 1
16. United Aircraft Research
 East Hartford, Connecticut
 Attention: Library 1
17. Detroit Diesel Allison Division
 Department 8894, Plant 8
 P. O. Box 894
 Indianapolis, Indiana 46206
 Attention: J. N. Barney 1
 G. E. Holbrook 1
 Library 1
18. Northern Research & Engineering Corp.
 219 Vassar Street
 Cambridge, Massachusetts 02139
 Attention: K. Ginwala 1
19. General Electric Company
 Flight Propulsion Division
 Cincinnati, Ohio 45215
 Attention: J. S. McBride H-44 1
 F. Burggraf H-32 1
 S. N. Suci H-32 1
 C. Danforth H-32 1
 Technical Information Center N-32 1
 D. Bahr 1
20. General Electric Company
 1000 Western Avenue
 West Lynn, Massachusetts 01905
 Attention: Dr. C. W. Smith
 Library Building 2-40M 1

21. Curtiss-Wright Corporation
Wright Aeronautical Division
Wood-Ridge, New Jersey 07075
Attention: D. Wagner 1
 W. Walker 1
22. Air Research Manufacturing Company
402 South 36th Street
Phoenix, Arizona 85034
Attention: Robert O. Bullock 1
23. Air Research Manufacturing Company
9851 Sepulveda Boulevard
Los Angeles, California 90009
Attention: Dr. N. Van Le 1
24. AVCO Corporation
Lycoming Division
550 South Main Street
Stratford, Connecticut
Attention: Claus W. Bolton 1
 Charles Kuintzie 1
25. Continental Aviation & Engineering Corporation
12700 Kercheval
Detroit, Michigan 48215
Attention: Eli H. Bernstein 1
 Howard C. Walch 1
26. International Harvester Company
Solar Division
2200 Pacific Highway
San Diego, California 92112
Attention: P. A. Pitt 1
 Mrs. L. Walper 1
27. Goodyear Atomic Corporation
Box 628
Piketon, Ohio
Attention: C. O. Langebrake 1
28. George Derderian AIR 53622 B
Department of the Navy
Bureau of the Navy
Washington, D. C. 20360 1

29. The Boeing Company
 Commercial Airplane Division
 P. O. Box 3991
 Seattle, Washington 98124
 Attention: G. J. Schott MS 80-66 1
30. The Boeing Company
 Missile and Information Systems Division
 224 N. Wilkinson Street
 Dayton, Ohio 45402
 Attention: Warren K. Thorson 1
31. Aerojet-General Corporation
 Sacramento, California 95809
 Attention: M. S. Nylin 1
 Library 1
32. Cornell Aeronautical Laboratory
 4455 Genessee Street
 Buffalo, New York 14221 1
33. Marquardt Corporation
 16555 Saticoy Street
 Van Nuys, California 1
34. Thompson Ramo Wooldridge
 23555 Euclid Avenue
 Cleveland, Ohio 1
35. ARO, Incorporated
 Arnold Air Force Station
 Tennessee 1
36. Professor J. M. Beer
 Dept. of Chem. Eng. & Fuel Tech.
 University of Sheffield,
 Mappin Street - Sheffield S1 3JD - Yorkshire
 Great Britain 1
37. Cummings Engine Co.
 Cummings Technical Center
 1900 McKinley Avenue
 Columbus, Indiana 47201
 Attention: Curt Dasbach
 Mail Code 50142 1

38. Garrett/AiResearch Co.
402 South 36th Street
Phoenix, Arizona 85034
Attention: John M. Haasis 1
39. Pratt & Whitney Aircraft
Florida Research & Development Center
Box 2691
West Palm Beach, Florida 33402
Attention: J. Chamberlain 1
J. Dykslag 1
J. Shadowen 1
G. Lewis 1
40. Professor A. H. Lefebre
The Cranfield Institute of Technology
Cranfield, Bedford
Great Britain 1
41. Aerojet General Corporation
Sacramento Facility
P. O. Box 15847
Sacramento, California 95813
Attention: C. E. Tedmon 1
Dave Kors 1
42. The University of Toledo
Toledo, Ohio 43606
Attention: Dr. Duen-Ten Jeng 1
Dr. Kenneth Dewitt 1
43. Eaton Yale and Towne Research Center
26201 Northwestern Highway
Southfield, Michigan 48075 1
44. Rocketdyne
North American Rockwell
6630 Canoga Avenue
Canoga Park, California 91304
Attention: S. D. Clapp
Manager
Propulsion Technology Research Division 1
45. Dept. of Mechanical Engineering
201 Engineering Building
Michigan State University
E. Lansing, Michigan 48823
Attention: Dr. Merle C. Potter 2